TauSpinner ALGORITHMS FOR INCLUDING SPIN AND NEW PHYSICS EFFECTS IN $\gamma\gamma \to \tau\tau$ PROCESS

A.Yu. Korchin a,b,c, E. Richter-Was c, Z. Was d

aNSC Kharkiv Institute of Physics and Technology, 61108 Kharkiv, Ukraine
 bV.N. Karazin Kharkiv National University, 61022 Kharkiv, Ukraine
 cM. Smoluchowski Institute of Physics, Jagiellonian University
 Łojasiewicza 11, 30-348 Kraków, Poland
 dInstitute of Nuclear Physics Polish Academy of Sciences
 Radzikowskiego 152, 31-342 Kraków, Poland

Received 22 August 2025, accepted 5 September 2025, published online 17 October 2025

The possible anomalous New Physics contributions to the electric and magnetic dipole moments of the τ lepton have brought renewed interest in development of new charge-parity violating signatures in the τ -pair production at Belle II energies, and also at higher energies of the LHC and the FCC. In this paper, we discuss the effects of anomalous contributions to the cross section and spin correlations in the $\gamma\gamma \to \tau^-\tau^+$ production processes, with τ decays included. Such processes have been observed in the pp and PbPb collisions at CERN LHC experiments. Due to the complex nature of the resulting distributions, Monte Carlo techniques are useful, in particular for event reweighting with studied New Physics phenomena. For the $\gamma\gamma$ processes, extensions of the Standard Model amplitudes are implemented in the TauSpinner program. This is mainly with the electric and magnetic dipole moments in mind, however the algorithm can easily be extended to other New Physics interactions, provided they can be encapsulated into the similar form-factors in the Standard Model structure of matrix elements. Basic formulas and algorithm principles are presented, and numerical examples are provided for illustration. Information on how to use the program is given in Appendix of the paper.

DOI:10.5506/APhysPolB.56.10-A4

1. Introduction

The electric and magnetic dipole moments of the τ lepton are sensitive to violation of fundamental symmetries, such as charge-parity (CP) violation [1–3]. Recent measurements of dipole moments of the τ lepton at the Belle experiment [4], as well as observation of $\gamma\gamma \to \tau^-\tau^+$ production at the hadron colliders [5, 6] had brought renewed interest in the electric

and magnetic dipole moments of the τ lepton. Deviation from the predicted and measured values of the magnetic moment of the muon [7], and possibly enhanced contributions from New Physics (NP) models to the magnetic moment of the τ lepton, proportional to the square of its mass, makes these studies important and of contemporary interest. Several beyond the Standard Model (SM) scenarios introduce dark weakly-interacting scalars or vector states accompanying production of heavy fermions, e.g. τ leptons, or through the loop corrections with new virtual particles, which can serve as a source of anomalous contributions to the electric or magnetic dipole moments of the τ lepton, as mentioned in [8, 9] and references therein.

In this paper, we discuss the effects on the cross section and spin correlations in the τ -pair production and decay. First, in the SM, because they determine the nature of interfering background for the impact of anomalous dipole moments and then the potential NP augmentation of dipole moments themselves. These studies include the calculation of the analytical formulas, implementation and validation in the tool, and presentation of impact on typical kinematic distributions. The impact of NP contributions to the dipole moments can be introduced on top of simulations of the $\gamma\gamma \to \tau^-\tau^+$ processes assuming the SM couplings, involving multi-body final states. The Monte Carlo (MC) solutions are convenient for this purpose and the calculations presented below have been implemented in the TauSpinner program for reweighting events with a τ pair produced in the pp or PbPb collisions.

The TauSpinner program [10, 11] is a convenient tool to study observables sensitive to the NP effects in hadron colliders. It allows us to include NP and spin effects in case they are absent in event samples generated with general purpose MC generators such as Pythia [12] or Sherpa [13]. Program development has a long history driven by the expanding scope of its initially designed applications [10]. First, the longitudinal spin effects in the case of Drell–Yan (Z, W) and Higgs decay processes of τ leptons at the LHC [10] were implemented. Later, it was extended to applications for the NP interactions in the hard processes, in which lepton pairs are accompanied by one or two hard jets [14], and to the transverse spin effects [15]. The implementations were then further extended to allow for the study of the electroweak effects in Refs. [16, 17] and the anomalous dipole moments of the τ -lepton couplings to vector bosons in Ref. [18]. In the present paper, we extend the calculations of Ref. [18] including the higher-order terms of the dipole moments in the case of $\gamma\gamma \to \tau\tau$ process and present more numerical results.

Let us introduce the terminology that is used throughout the paper. In the $\gamma\gamma \to \tau^-\tau^+$ reaction with real photons, we include the anomalous magnetic and electric dipole moments of the τ lepton as form-factors. At the real-photon point, $q^2=0$, the electromagnetic form-factors reduce to the corresponding dipole moments. These form-factors are connected to the

chirality flipping operators. The terms proportional to the electric form-factor are also CP-violating. In general, the magnetic form-factor has a contribution from radiative corrections in the SM, and we separate this contribution from the NP term. As for the electric dipole form-factor, it is highly suppressed in the SM, and one can assume that this form-factor comes exclusively from NP.

Our paper is organized as follows. In Section 2, we present analytical results for the spin-correlation matrix including the effects of the τ -lepton anomalous magnetic and electric dipole form-factors, the SM and NP ones. In Section 3, we recall the main points of the TauSpinner reweighting algorithms for the inclusion of dipole moments. Discussions on some numerical results are collected in Section 4. First, elements of the spin-correlation matrix are shown in Subsection 4.1, and we discuss the main features of the $\gamma\gamma \to \tau^-\tau^+$ process spin correlations. Then, in Subsection 4.2, the impact of spin correlations in the SM and NP extensions on typical kinematical distributions in the case of both $\tau^{\pm} \to \pi^{\pm} \nu_{\tau}$ decays is shown. It is followed by similar discussions of the case with both $\tau^{\pm} \to \pi^{\pm} \pi^{0} \nu_{\tau}$ in Subsection 4.3, and in the case of one τ decaying $\tau^{\pm} \to \mu^{\pm} \nu_{\tau} \nu_{\mu}$ and another τ decaying $\tau^{\mp} \to \pi^{\mp} \nu_{\tau}$ in Subsection 4.4. The paper closes with summary and outlook in Section 5. Technical description of TauSpinner initialisation and available weights is given in Appendix A, and expressions for the elements of the spin-correlation matrix used in the code are listed in Appendix B.

2. Amplitudes and spin correlations

In this section, the formulas for the two-photon production of the polarised τ leptons, $\gamma\gamma \to \tau^-\tau^+$, are considered. In [18, 19], we discussed the formulas for including the magnetic and electric dipole form-factors in elementary $2\to 2$ parton processes of τ -pair production. Here, we extend the formulas for the $\gamma\gamma \to \tau^-\tau^+$ process to include also higher-order terms in the dipole moments.

For the sake of a smoother read, let us first recall the introduction presented in [18]. The spin amplitude for the $AB \to \tau^+\tau^-$ process with $AB = \gamma\gamma$ can be written as follows:

$$A(k_1) + B(k_2) \to \tau^-(p_-) + \tau^+(p_+)$$
 (1)

with the four-momenta satisfying $k_1 + k_2 = p_- + p_+$.

In the center-of-mass (CM) frame, the components of the momenta are

$$p_{-} = (E, \vec{p}), p_{+} = (E, -\vec{p}), \vec{p} = (0, 0, p),$$

 $k_{1} = (E, \vec{k}), k_{2} = (E, -\vec{k}), \vec{k} = (E \sin \theta, 0, E \cos \theta), (2)$

so that the $\hat{3}$ axis is along the momentum \vec{p} , the reaction plane is spanned on the $\hat{1}$ and $\hat{3}$ axes defined by the momenta \vec{p} and \vec{k} , and the $\hat{2}$ axis is along $\vec{p} \times \vec{k}$. Here, $E = \frac{1}{2}\sqrt{s}$ is the photon (τ lepton) energy, $p = \beta E$ is the τ -lepton three-momentum, where $\beta = (1 - 4\frac{m_{\tau}^2}{\epsilon})^{1/2}$ is the velocity, and m_{τ} is the mass of the τ lepton. The quantization frames of τ^- and τ^+ are connected to this reaction frame by the appropriate boosts along the $\hat{3}$ direction. Note that the $\hat{3}$ axis is parallel to the momentum of τ^- but anti-parallel to the momentum of τ^+ . Only the reaction frame, the τ^- and the τ^+ rest frames are used for calculations throughout the paper.

We assume that the $\gamma\tau\tau$ electromagnetic vertex has the following structure:

$$\Gamma_{\gamma}^{\mu}(q) = -ieQ_{\tau} \left\{ \gamma^{\mu} F_{1}\left(q^{2}\right) + \frac{\sigma^{\mu\nu} q_{\nu}}{2m_{\tau}} \left[iA\left(q^{2}\right) + B\left(q^{2}\right)\gamma_{5} \right] \right\}, \quad (3)$$

where q is the photon four-momentum, e is the positron charge, $Q_{\tau} = -1$, $\sigma^{\mu\nu} = \frac{i}{2}[\gamma^{\mu}, \gamma^{\nu}], F_1(q^2)$ is the Dirac form-factor, $A(q^2) = F_2(q^2)$ is the Pauli form-factor, and $B(q^2) = F_3(q^2)$ is the electric dipole form-factor. At the real-photon point, $F_1(0) = 1$, A(0) is the anomalous magnetic dipole moment a_{τ} , and B(0) is related to the CP-violating electric dipole moment d_{τ}

$$A(0) = a_{\tau}, \qquad B(0) = \frac{2m_{\tau}}{eQ_{\tau}} d_{\tau}.$$
 (4)

In the description of the $\gamma(k_1) + \gamma(k_2) \to \tau^-(p_-) + \tau^+(p_+)$ reaction with the real photons $(k_1^2 = k_2^2 = 0)$, we separate the contribution from NP including the total SM contribution $A(0)_{\rm SM} = 1.17721(5) \times 10^{-3}$ [9], and define

$$A(0) = A(0)_{SM} + A(0)_{NP}, \qquad B(0) = B(0)_{NP}$$
 (5)

neglecting the minor contribution to B(0) in the SM. We assume that for the real photons, the dipole moments are real-valued.

After squaring the matrix element in the order e^2 and averaging the result over the polarisations of the photons, we obtain

$$|\mathcal{M}|^2 = \sum_{i,j=1}^4 R_{ij} \, s_i^- s_j^+ = R_{44} + \sum_{i,j=1}^3 R_{ij} \, s_i^- s_j^+, \tag{6}$$

where $s_i^{\mp} \equiv (\vec{s}^{\mp}, 1)$, and elements $R_{4i} = R_{i4} = 0$ for i = 1, 2, 3. The s_i^-, s_j^+ represent spin density states of the outgoing τ^-, τ^+ , respectively¹. The elements of the spin-correlation matrix R_{ij} depend on the

¹ In the earlier version of the code, we kept in R_{ij} only terms linear in the dipole moments, as published in [18]. Here, we include the higher-order terms as well, which allows one to study the impact on the total cross section from NP models for B.

invariant mass of the τ pair $m_{\tau^+\tau^-} = \sqrt{s}$ and the scattering angle θ . They are written below in terms of the velocity β , Lorentz factor $\gamma = \sqrt{s}/(2m_{\tau})$, and θ .

Elements R_{ij} , in the form as used in the TauSpinner code, are explicitly given in Appendix B. A more convenient representation of R_{ij} is an expansion in powers of A and B (here $A \equiv A(0)$ and $B \equiv B(0)$)

$$R_{ij} = \frac{e^4}{(1 - \beta^2 \cos^2 \theta)^2} \sum_{m, n=0 \, (m+n \le 4)}^4 A^m B^n c_{mn}^{(ij)} \qquad (i, j = 1, 2, 3, 4) \,. \quad (7)$$

The nonzero coefficients $c_{mn}^{(ij)}$ are presented below.

For the transverse–transverse spin-diagonal elements R_{11} , we obtain

$$\begin{split} c_{00}^{(11)} &= \frac{1}{8} \left[22\beta^2 - 11\beta^4 - \beta^2 \left(\beta^2 - 2 \right) \left(-4\cos 2\theta + \cos 4\theta \right) - 8 \right] \,, \\ c_{10}^{(11)} &= \frac{1}{2} \left(7\beta^2 + \beta^2 \cos 4\theta - 8 \right) \,, \\ c_{20}^{(11)} &= -\frac{1}{4} \gamma^2 \left\{ 20 - 35\beta^2 + 12\beta^4 + \beta^2 \left[\left(6\beta^2 - 2 \right) \cos 2\theta \right. \right. \\ &\left. + \left(2\beta^2 - 3 \right) \cos 4\theta \right] \right\} \,, \\ c_{30}^{(11)} &= c_{12}^{(11)} = -\frac{1}{4} \gamma^2 \left[8 - 14\beta^2 + 3\beta^4 + 4\beta^4 \cos 2\theta + \beta^2 \left(\beta^2 - 2 \right) \cos 4\theta \right] \,, \\ c_{40}^{(11)} &= c_{04}^{(11)} = \frac{1}{2} c_{22}^{(11)} \\ &= \frac{1}{128} \gamma^4 \left\{ 6\beta^2 \left(\beta^2 - 8 \right) \left(\beta^2 - 2 \right) + \beta^2 \left[\left(17\beta^4 - 16\beta^2 - 16 \right) \cos 2\theta \right. \\ &\left. + 2 \left(8 + 5\beta^2 \left(\beta^2 - 2 \right) \right) \cos 4\theta - \beta^4 \cos 6\theta \right] - 32 \right\} \,, \\ c_{02}^{(11)} &= \frac{1}{2} \left[6 \left(\beta^2 - 1 \right) + \beta^2 \left(\cos 4\theta - \cos 2\theta \right) \right] \,, \end{split} \tag{8}$$

and for the transverse–transverse spin-diagonal element R_{22} , we have

$$c_{00}^{(22)} = 2\beta^2 - 2\beta^4 - \beta^4 \cos^2 \theta \left(\cos^2 \theta - 2\right) - 1,$$

$$c_{10}^{(22)} = -4\left(1 - \beta^2 \cos^2 \theta\right),$$

$$c_{20}^{(22)} = -5\left(1 - \beta^2 \cos^2 \theta\right),$$

$$c_{30}^{(22)} = c_{12}^{(22)} = -2\left(1 - \beta^2 \cos^2 \theta\right),$$

$$c_{40}^{(22)} = c_{04}^{(11)} = \frac{1}{2}c_{22}^{(11)}$$

$$= -\frac{1}{4}\gamma^4 \left(1 - \beta^2 \cos^2 \theta\right) \left[1 - 2\beta^2 + 2\beta^4 + \beta^4 \cos^2 \theta \left(\cos^2 \theta - 2\right)\right],$$

$$c_{02}^{(22)} = -\gamma^2 \left[3 - 5\beta^2 + 4\beta^4 - \left(\beta^2 + 3\beta^4\right) \cos^2 \theta + 2\beta^4 \cos^4 \theta\right]. \tag{9}$$

For the transverse–transverse spin-nondiagonal element R_{12} , the coefficients are

$$\begin{split} c_{01}^{(12)} &= \frac{1}{4}\beta \left(15\beta^2 + 4\cos 2\theta + \beta^2\cos 4\theta - 20\right) \,, \\ c_{03}^{(12)} &= c_{21}^{(12)} = -\frac{1}{2}\beta\gamma^2 \left(2 - 3\beta^2 + \beta^2\cos 2\theta\right)\sin^2\theta \,, \\ c_{11}^{(12)} &= -\frac{1}{4}\beta\gamma^2 \left[12 - 19\beta^2 + 4\beta^4 + 4\left(\beta^4 + \beta^2 - 1\right)\cos 2\theta - \beta^2\cos 4\theta\right] \,. \,(10) \end{split}$$

Next, we present coefficients for the longitudinal–longitudinal element R_{33} as

$$c_{00}^{(33)} = -1 + 2\beta^4 + \beta^2 \cos^2 \theta \left[2 - 2\beta^2 + (\beta^2 - 2) \cos^2 \theta \right],$$

$$c_{10}^{(33)} = \frac{1}{2} \left(-8 + 9\beta^2 - \beta^2 \cos 4\theta \right),$$

$$c_{20}^{(33)} = -\gamma^2 \left\{ 5 - 5\beta^2 + 2\beta^4 + \beta^2 \cos^2 \theta \left[-8 + 5\beta^2 + (3 - 2\beta^2) \cos 2\theta \right] \right\},$$

$$c_{30}^{(33)} = c_{12}^{(33)} = -\gamma^2 \left[2 - \beta^2 (\beta^2 - 2) \cos^2 \theta (\cos 2\theta - 3) \right],$$

$$c_{40}^{(33)} = c_{04}^{(33)} = \frac{1}{2} c_{22}^{(33)}$$

$$= \frac{1}{4} \gamma^4 \left\{ -1 + 2\beta^4 + \beta^2 \cos^2 \theta \left[7 + 2\beta^2 (\beta^2 - 6) + (7\beta^2 - 4) \cos^2 \theta - \beta^4 \cos^4 \theta \right] \right\},$$

$$c_{02}^{(33)} = -\gamma^2 \left\{ 3 - \beta^2 + \beta^2 \cos^2 \theta \left[-9 + 5\beta^2 - 2(\beta^2 - 2) \cos^2 \theta \right] \right\}. \tag{11}$$

There are the nonzero longitudinal–transverse elements R_{13} and R_{23} with the coefficients

$$c_{00}^{(13)} = \frac{\beta^2}{\gamma} \sin^2 \theta \sin 2\theta ,$$

$$c_{10}^{(13)} = \beta^2 \gamma \left[1 + (\beta^2 - 2) \cos^2 \theta \right] \sin 2\theta ,$$

$$c_{20}^{(13)} = \frac{1}{2} \beta^2 \gamma \left[5 + (\beta^2 - 6) \cos^2 \theta \right] \sin 2\theta ,$$

$$c_{30}^{(13)} = c_{12}^{(13)} = 2\beta^2 \gamma \sin^2 \theta \sin 2\theta ,$$

$$c_{40}^{(13)} = c_{04}^{(13)} = \frac{1}{2} c_{22}^{(13)} = \frac{1}{2} \beta^2 \gamma \sin^2 \theta \sin 2\theta ,$$

$$c_{02}^{(13)} = \frac{1}{2} \beta^2 \gamma \left[5 - 2\beta^2 + (\beta^2 - 4) \cos^2 \theta \right] \sin 2\theta ,$$

$$(12)$$

and

$$c_{01}^{(23)} = c_{11}^{(23)} = 2c_{03}^{(23)} = 2c_{21}^{(23)}$$
$$= \frac{1}{2}\beta\gamma \left(2 - 3\beta^2 + \beta^2\cos 2\theta\right)\sin 2\theta. \tag{13}$$

For the spin-independent element R_{44} , the nonzero coefficients $c_{mn}^{(44)}$ read

$$\begin{split} c_{00}^{(44)} &= 1 + 2\beta^2 - 2\beta^4 - 2\beta^2 \left(1 - \beta^2\right) \cos^2 \theta - \beta^4 \cos^4 \theta \,, \\ c_{10}^{(44)} &= 4 \left(1 - \beta^2 \cos^2 \theta\right) \,, \\ c_{20}^{(44)} &= \frac{1}{2} \gamma^2 \left(\beta^2 + \beta^2 \cos 2\theta - 2\right) \left(3\beta^2 + 2\beta^2 \cos 2\theta - 5\right) \,, \\ c_{30}^{(44)} &= c_{12}^{(44)} = \gamma^2 \left(\beta^2 \cos 2\theta - 1\right) \left(\beta^2 + \beta^2 \cos 2\theta - 2\right) \,, \\ c_{40}^{(44)} &= c_{04}^{(44)} = \frac{1}{2} c_{22}^{(44)} \\ &= \frac{1}{4} \gamma^4 \left(1 - \beta^2 \cos^2 \theta\right) \left[1 + 2\beta^2 - 2\beta^4 + 2\beta^2 \left(\beta^2 - 2\right) \cos^2 \theta + \beta^4 \cos^4 \theta\right] \,, \\ c_{02}^{(44)} &= -\gamma^2 \left(1 - \beta^2 \cos^2 \theta\right) \left(\beta^2 + 2\beta^2 \cos 2\theta - 3\right) \,. \end{split}$$

The following symmetry relations are fulfilled: $R_{21} = -R_{12}$, $R_{31} = R_{13}$, and $R_{32} = -R_{23}$.

Note that the formulas published in [18] correspond to keeping only coefficients $c_{00}^{(ij)}$, $c_{10}^{(ij)}$, and $c_{01}^{(ij)}$ in Eqs. (8)–(14). The expressions in the present paper include the higher-order terms in dipole moments A and B up to the power of 4. In particular, R_{44} depends not only on A but also on B^2 and B^4 , allowing in experimental analysis to study the impact of the electric dipole moment on the cross section summed over all spin density configurations. Also, the contribution from the electric dipole moment is no longer different from the rest of the terms, as was the case of [18], where only R_{23} and R_{12} were dependent on B, while all other elements R_{ij} were dependent on A only.

Finally, the cross section of the $\gamma\gamma \to \tau^-\tau^+$ process is expressed as

$$\frac{\mathrm{d}\sigma}{\mathrm{d}\Omega} \left(\gamma \gamma \to \tau^- \tau^+ \right) = \frac{\beta}{64\pi^2 s} \left(R_{44} + \sum_{i,j=1}^3 R_{ij} \, s_i^- s_j^+ \right) \,. \tag{15}$$

The element R_{44} determines the cross section in which the sum is taken over the spins of the τ leptons²

$$\frac{\mathrm{d}\sigma}{\mathrm{d}\Omega} \left(\gamma \gamma \to \tau^- \tau^+ \right) = \frac{\beta}{16\pi^2 s} R_{44} \,. \tag{16}$$

One can further rearrange Eq. (15) and introduce the normalized elements $r_{ij} = R_{ij}/R_{44}$, factorizing out explicitly the spin-correlation compo-

² Note that in the SM, the one-loop electroweak corrections to the cross section of the $\gamma\gamma \to \mu^-\mu^+$ and $\gamma\gamma \to \tau^-\tau^+$ processes with unpolarized leptons have been calculated in Ref. [20].

nents of the cross section

$$\frac{d\sigma}{d\Omega} \left(\gamma \gamma \to \tau^- \tau^+ \right) = \frac{\beta}{64\pi^2 s} \, R_{44} \, \left(r_{44} + \sum_{i,j=1}^3 r_{ij} \, s_i^- s_j^+ \right) \,, \qquad r_{44} = 1 \,.$$
(17)

Let us stress now that the frame and sign convention of R_{ij} presented in Eqs. (8)–(14) differ from the ones used later in the paper, and in the TauSpinner program, when the matrix is contracted with τ -lepton polarimetric vectors. The change in convention reads as follows:

$$R_{tt} \leftarrow R_{44}, \quad R_{tx} \leftarrow -R_{42}, \quad R_{ty} \leftarrow -R_{41}, \quad R_{tz} \leftarrow -R_{43},$$
 $R_{xt} \leftarrow -R_{24}, \quad R_{xx} \leftarrow R_{22}, \quad R_{xy} \leftarrow R_{21}, \quad R_{xz} \leftarrow R_{23},$
 $R_{yt} \leftarrow -R_{14}, \quad R_{yx} \leftarrow R_{12}, \quad R_{yy} \leftarrow R_{11}, \quad R_{yz} \leftarrow R_{13},$
 $R_{zt} \leftarrow -R_{34}, \quad R_{zx} \leftarrow R_{32}, \quad R_{zy} \leftarrow R_{31}, \quad R_{zz} \leftarrow R_{33}.$ (18)

Let us briefly explain that there are several reasons for the frame orientation differences used in the TauSpinner and TAUOLA decay library [21]. Historical one; in the past, reactions were organized with the z axis along e^+ or antiquark direction, whereas now, many authors prefer to use the z axis along e^- or quark directions. This was the convention used for the KKMC [22] and TAUOLA [21] programs implementations. To adjust, this require π angle rotation around an axis usually perpendicular to the reaction plane. There is also an overall sign which is affecting τ^+ spin indices of the spin-correlation matrices. This is moved in all TAUOLA/TauSpinner interfaces [23] from the τ decay to spin-correlation matrices. Also, for many past calculations which we rely on as reference, the rest frames of τ^{\pm} were chosen to have the common z-axis direction, parallel to the z axis of the reaction frame (where incoming partons do not define z direction). For calculations involving NP, we have found that for present-day authors, it is most convenient to allow for distinct frame orientations rather than that. The easiest way to solve this different conventions was to provide for the TauSpinner implementation an adjustment internal routine.

There is also another adjustment, this time for the τ^+ polarimetric vector orientation, as well as its overall sign. At present, this adjustment is shifted into R_{ij} matrix redefinition too³, even though it does not correspond to a change of its orientation, but is for the τ^+ polarimetric vector. Finally,

³ It is done separately, in the different place in the code, just before the event weight calculation.

$$R_{tt} = R_{44}, \quad R_{tx} = -R_{42}, \quad R_{ty} = -R_{41}, \quad R_{tz} = -R_{43},$$

$$R_{xt} = -R_{24}, \quad R_{xx} = R_{22}, \quad R_{xy} = R_{21}, \quad R_{xz} = R_{23},$$

$$R_{yt} = R_{14}, \quad R_{yx} = -R_{12}, \quad R_{yy} = -R_{11}, \quad R_{yz} = -R_{13},$$

$$R_{zt} = -R_{34}, \quad R_{zx} = R_{32}, \quad R_{zy} = R_{31}, \quad R_{zz} = R_{33}. \quad (19)$$

With this transformation, expressions of the R_{ij} matrices of Eq. (19) with i, j = t, x, y, z are used in the TauSpinner event reweighting algorithm discussed in Section 3 for calculating weight implemented in the TauSpinner code and in Section 4 for presenting numerical results.

3. The reweighting algorithm for TauSpinner

The basis formalism of TauSpinner is documented in Ref. [11], Section 2.2, Eqs. (7) to (12). We do not repeat here the details of this formalism nor explain how kinematics of the hard process is deciphered from kinematics of the τ -decay products. We recall however a few basic equations for calculating final weights, which allow one to take into account the changes in the cross section and spin correlations in the SM and SM+NP models.

The basic equation in the calculation of the cross section is

$$d\sigma = \sum_{\text{flavors}} \int dx_1 dx_2 f(x_1, ...) f(x_2, ...) d\Omega_{\text{prod}}^{\text{parton level}} d\Omega_{\tau^+} d\Omega_{\tau^-}$$

$$\times \left(\sum_{\lambda_1, \lambda_2} \left| \mathcal{M}_{\text{parton level}}^{\text{prod}} \right|^2 \right) \left(\sum_{\lambda_1} \left| \mathcal{M}^{\tau^+} \right|^2 \right) \left(\sum_{\lambda_2} \left| \mathcal{M}^{\tau^-} \right|^2 \right) wt_{\text{spin}}, (20)$$

where x_1, x_2 denote fractions of the beam momenta carried by the partons, $f(x_1, ...), f(x_2, ...)$ are parton distribution functions (PDF)s of the beams⁴, and $d\Omega$ denote phase-space integration elements. Equation (20) represents the product of distribution for the τ^{\pm} production and decay, $(\sum_{\lambda_i} |\mathcal{M}^{\tau^{\pm}}|^2)$ stands for the decay matrix element squared, and $(\sum_{\lambda_1,\lambda_2} |\mathcal{M}^{\text{prod}}_{\text{parton level}}|^2)$ stands for the production matrix element squared. Only the spin weight wt_{spin} needs input both from τ^{\pm} production and decay.

The R_{ij} used in the calculation of components of Eq. (20) are taken as a weighted average (with PDFs and production matrix elements squared) over all flavour configurations, as in the following equation:

⁴ The TauSpinner algorithm does not use information about the flavour of incoming partons from the event record, allowing for the application of its weight also on experimental data.

$$R_{ij} \to \frac{\sum_{\text{flav}} f(x_1, ...) f(x_2, ...) \left(\sum_{\lambda_1, \lambda_2} \left| \mathcal{M}_{\text{parton level}}^{\text{prod}} \right|^2 \right) R_{ij}}{\sum_{\text{flav}} f(x_1, ...) f(x_2, ...) \left(\sum_{\lambda_1, \lambda_2} \left| \mathcal{M}_{\text{parton level}}^{\text{prod}} \right|^2 \right)}.$$
(21)

No approximation is introduced in this way; the denominator of Eq. (21) cancels explicitly the corresponding factor of Eq. (20).

For the $wt_{\rm spin}$ calculation, the normalised elements $r_{ij} = R_{ij}/R_{tt}$ are used, following Eq. (17),

$$wt_{\text{spin}} = \sum_{i,j=t,x,y,z} r_{ij} h_{\tau^{+}}^{i} h_{\tau^{-}}^{j}.$$
 (22)

Here, $h_{\tau^+}^i$, $h_{\tau^-}^j$ stand for decay mode-dependent τ^+ , τ^- polarimetric vectors. This weight is the only term which needs input from both τ^{\pm} production and decay. Please note that the $wt_{\rm spin}$ is independent of the PDFs, except through already averaged over partons contribution r_{ij} elements of the spin-correlations matrix which are used.

To introduce the corrections due to different spin effects and modified production process in the generated sample (*i.e.* without re-generation of events), one can define the weight wt, representing the ratio of the new-to-old cross sections at each point in the phase space.

Equation (20) for the modified cross section takes then the form

$$d\sigma_{new} = d\sigma_{old} \ w t_{prod}^{new/old} \ w t_{spin}^{new/old}, \qquad (23)$$

where $\sigma_{\rm old}$ is calculated with Eq. (16), $wt_{\rm spin}$ using Eq. (22) and $wt_{\rm prod}^{\rm new/old}$ using Eq. (24) below

$$wt_{\text{prod}}^{\text{new/old}} = \frac{\sum_{\text{flav}} f(x_1, ...) f(x_2, ...) \left(\sum_{\text{spin}} \left| \mathcal{M}_{\text{part.lev.}}^{\text{prod}} \right|^2\right) \Big|_{\text{new}}}{\sum_{\text{flav}} f(x_1, ...) f(x_2, ...) \left(\sum_{\text{spin}} \left| \mathcal{M}_{\text{part.lev.}}^{\text{prod}} \right|^2\right) \Big|_{\text{old}}} = \frac{R_{tt}|_{\text{new}}}{R_{tt}|_{\text{old}}}.$$
(24)

The present implementation assumes that the generated sample has no spin correlations included, however, it can easily be extended⁵ to provide a weight calculated as

$$wt_{\text{spin}}^{\text{new/old}} = \frac{\sum_{i,j=t,x,y,z} r_{ij} h_{\tau^{+}}^{i} h_{\tau^{-}}^{j} \Big|_{\text{new}}}{\sum_{i,j=t,x,y,z} r_{ij} h_{\tau^{+}}^{i} h_{\tau^{-}}^{j} \Big|_{\text{old}}}.$$
 (25)

⁵ Such a special case is available for $\bar{q}q \to \tau\tau$ processes, where, for example, polarisation but not spin correlations was included in the generated sample.

The TauSpinner program provides both weights, $wt_{\rm spin}$ and $wt_{\rm prod}$, which allow one to modify per-event distributions of the sample generated according to the ${\rm d}\sigma_{\rm old}$ model and should be used as multiplicative components.

The combined weight should be used as a multiplicative product as in Eq. (26) $wt = wt_{\text{prod}}^{\text{new/old}} \times wt_{\text{spin}}^{\text{new/old}}, \qquad (26)$

where the first term of the weight represents the modification of the matrix elements for production, the second term — of the spin correlations. It is nothing more than ratios of spin-averaged amplitudes squared for the whole process; new to old. If the analysis is sensitive to changes in the PDFs parametrisations used for sample generation and TauSpinner weights calculations, it should be taken into account in the calculation of $wt_{\rm prod}^{\rm new/old}$ and $wt_{\rm spin}^{\rm new/old}$ in Eq. (26). If the production process is not modified, $wt_{\rm prod}^{\rm new/old}$ is equal to 1. For the sample originally generated without spin correlations, $wt_{\rm spin}^{\rm new/old}$ alone allows us to introduce the desired spin effects.

In Eq. (24), indirectly through (21), also in (25), \sum_{flav} stands for including all components of the beam which lead to the τ pair in the final state being produced. For calculating weights of the $\gamma\gamma \to \tau^-\tau^+$ events, the sum over flavours includes now also photons. This requires, on one side, structure functions available for the quasi-real photon as a parton in the proton or heavy ion, and, on the other side, the t- and u-channels matrix element for the $\gamma\gamma \to \tau^-\tau^+$ hard process, with the spin correlations included.

Let us now give more technical details on the implementation for the $\gamma\gamma \to \tau\tau$ process. The $\gamma\gamma \to \tau^-\tau^+$ hard process, its spin amplitudes, cross section, and spin-correlation matrix were described in Section 2. The non-normalized spin-correlation matrix R_{ij} of Eq. (19) contains all the necessary information for calculating the cross sections and introducing spin-correlation effects in the $\gamma\gamma \to \tau^-\tau^+$ events. Each parton process contributes incoherently to the final state. That is why introduction of a nearly real photon as an extra parton, and a corresponding hard process, were possible with a straightforward extension of the sums in Eq. (20). As for the set of the PDFs, in the case of pp collision, one could take the ones described, e.g. in Refs. [24, 25]. These structure functions include the photon PDF as well. Alternatively, and that is our choice recommended for the PbPb collision, where a parametrisation of the photon flux is not easily available, we can simply request that $\gamma\gamma$ contributes in proportion to all other processes.

In the present implementation, the $\tau\tau$ events are analyzed as if they were produced through a combination of parton level $\bar{q}q$ and $\gamma\gamma$ processes, and that they contribute in the proportion to quark processes set by the user⁶. This can be changed and the corresponding photon PDFs can be installed.

⁶ Parameters GAMfraci and GAMfrac2i are set at the initialisation step.

At present, the R_{ij} elements of $\bar{q}q$ part are averaged over all parton flavours according to the density obtained from the PDFs library. Then the contribution from the $\gamma\gamma$ process to R_{ij} is added with a fixed proportion to the ones of quarks. This may look like an oversimplification, but we firstly avoid evaluating the γ PDFs variants, as the γ PDFs may be strongly dependent on the experimental conditions. Secondly, it gives the flexibility in using TauSpinner weights for the $\gamma\gamma \to \tau\tau$ produced in PbPb collisions, where the issue of incoming photon fluxes is modeled with specialized MC generators and is sensitive to experimental conditions. In fact, we assume that the case, in which only the $\gamma\gamma$ process contributes, is unphysical, as there are always accompanying processes from the $\bar{q}q$ interactions, also in the PbPb beam case. Nevertheless, user interested in such a case can always set parameters GAMfraci, GAMfrac2i to very large values, so that the quark process contribution is much smaller than the measurements ambiguity threshold.

4. Numerical results

Numerical results presented below are based on events generated with Pythia 8.3 [12] using pp scattering at 13 TeV, hard process PhotonCollision:gmgm2tautau, internal parametrisation of structure functions PDF:pSet = 13, and restricted to a low mass range of the $\tau\tau$ pair, $m_{\tau\tau}=5$ –50 GeV and $p_{\rm T}^{\tau\tau}>5$ GeV. This choice of phase-space corresponds roughly to the range covered by the $\gamma\gamma\to\tau\tau$ processes in PbPb collisions at the LHC. Then, the τ decays were modeled with the TAUOLA decay library [21] with no spin correlations between decaying τ leptons assumed. In total, we have available about 0.8×10^6 events for each decay mode combination generated. Then, the spin correlations were added using the weight calculated with the TauSpinner program discussed in Section 3, both for the spin-correlation effects in the SM and SM+NP models, and the cross-section normalisation in SM+NP models.

In Fig. 1, distributions of invariant mass $m_{\tau\tau}$ and $\cos\theta$ of the scattering angle for the generated sample are shown. Using the weight calculated with TauSpinner, the distributions are shown for the SM and two SM+NP models: $A=0.02,\ B=0.0$ and $A=0.0,\ B=0.02$. The effect of the NP models on these distributions is small and will be quantified with Table 1 discussed later. The τ leptons decay in the following decay mode configurations: both $\tau \to \pi \nu_{\tau}$, both $\tau \to \rho \nu_{\tau}$, and one $\tau \to \mu \nu_{\tau} \nu_{\mu}$ with another one $\tau \to \pi \nu_{\tau}$.

In the following, we discuss numerical results for elements of the spincorrelation matrix R_{ij} and identify which component may be the most sensitive to dipole moments and provide some evidence of NP. Then we move to discussing the impact on a few kinematical variables, typically studied in the experimental analysis. The aim is to quantify the effect of spin correlations as present in the SM and then the impact from NP extensions due to the anomalous dipole moments.

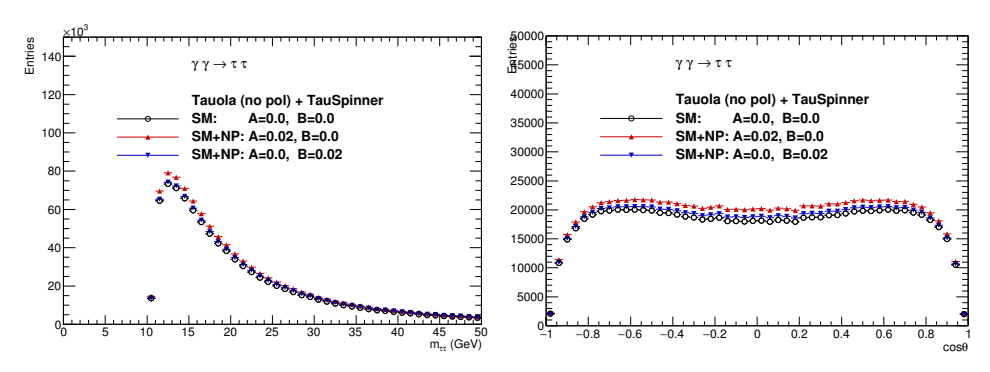


Fig. 1. Distribution of invariant mass of the $\tau\tau$ system and $\cos\theta$ of the scattering angle for the analyzed sample of the $\gamma\gamma \to \tau\tau$ events.

4.1. Spin-correlation elements R_{ij}

To simplify discussion, we use as a reference the SM with A=B=0. It is assumed that for the application, dipole moments due to the SM loop corrections are small and will be dropped out when discussing the NP effects. Therefore, for numerical results, we compare the SM predictions with six different settings for the dipole moments: (i) $A=0.002,\,0005,\,0.02$ with $B=0,\,$ and (ii) A=0 with $B=0.002,\,0.005,\,0.02$. This choice is somewhat arbitrary, covering the range which is plausible and behaving numerically stable with higher powers of A and B terms included. The smallest considered value, A=0.002, roughly corresponds to $2\times A_{\rm SM}$.

Impact on the cross section is quantified in Table 1. For the same values of anomalous A and B, the impact on the cross section is a few times bigger (of the order of 5) from A than from B, being about 0.6% for A=0.002 corresponding to $\sim 2\times A_{\rm SM}$, and about 9% for A=0.02 corresponding to $\sim 20\times A_{\rm SM}$. Correspondingly, the impact of B is below 0.1% for B=0.002, and 3% for B=0.02.

Table 1. The $\sigma^{\rm SM+NP}/\sigma^{\rm SM}$ for scan of different SM+NP models.

NP model	$\sigma^{ m SM+NP}/\sigma^{ m SM}$
A = 0.002; B = 0.0	1.006 ± 0.001
A = 0.005; B = 0.0	1.017 ± 0.001
A = 0.020; B = 0.0	1.091 ± 0.001
A = 0.0; B = 0.002	1.000 ± 0.001
A = 0.0; B = 0.005	1.002 ± 0.001
A = 0.0; B = 0.020	1.030 ± 0.001

Let us remind that we expect the effect of the NP extension of the SM to be very small, given the plausible range of the parameters A and B. But the spin correlations in the SM should not be neglected in the first place when extracting limits from experimental data analysis.

Figure 2 shows the distribution of R_{tt} as a function of $m_{\tau\tau}$ (top plots), restricted to the range of $\theta = \pi/3 \times [0.8 - 1.2]$ (middle plots) and restricted to $\theta = 2\pi/3 \times [0.8 - 1.2]$ (bottom plots). By construction, for the SM, R_{tt} is chosen 1.0, and it increases with the NP dipole moments. The element R_{tt} is more sensitive to changes in the magnetic dipole moment A than in the electric one B, and for both, the sensitivity increases with increasing the invariant mass of the $\tau\tau$ system. We observe that the effects are larger and of the same sign for the middle and bottom plots than for the top one, which is integrated over the full range of θ . This indicates that regions of θ close to $\pi/2$ are of lesser sensitivity to A and B. At the highest mass point studied, $m_{\tau\tau} = 50$ GeV, and integrated over the full phase space, R_{tt} reaches about 20\% for A = 0.02 and 10\% for B = 0.02. When restricting the scattering angle to the range of $\theta = \pi/3 \times [0.8 - 1.2]$, the effect is magnified, reaching 25\% and 15\%, respectively. In the opposite hemisphere, $\theta = 2\pi/3 \times [0.8 -$ 1.2], the effect is even larger, about 35% and 25%, respectively, indicating some asymmetry which can be explored further with experimental analysis. Note, however, that such significant effects are observed for non-realistically large values of A and B.

Figure 3 shows elements $r_{ij} = R_{ij}/R_{tt}$ in the SM and the discussed above SM+NP models. The diagonal elements of r_{ij} are sizable (top and middle lines), in the bottom line shown is the r_{xy} element, in which the SM contributions are close to zero but the NP ones are not. In the left column, the effect of varying A is shown, in the right column, the effect of varying B. For A=0.02, some shift is observed on r_{yy} , largely independent of $m_{\tau\tau}$. For B=0.02, the largely independent of $m_{\tau\tau}$ effect is visible in r_{xy} (which has zero contribution from the SM) and some effect on r_{zz} at the higher end of the studied $m_{\tau\tau}$ range. The other non-diagonal elements r_{ij} have nearly zero SM contributions, then the dipole moment contributions are tiny as well. That is why we have dropped out r_{zx} and r_{zy} plots.

In Figs. 4, 5, we show the effect of r_{ij} as a function of $\cos \theta$. These plots help to identify details of anomalous coupling dependence, which were observed in Fig. 2.

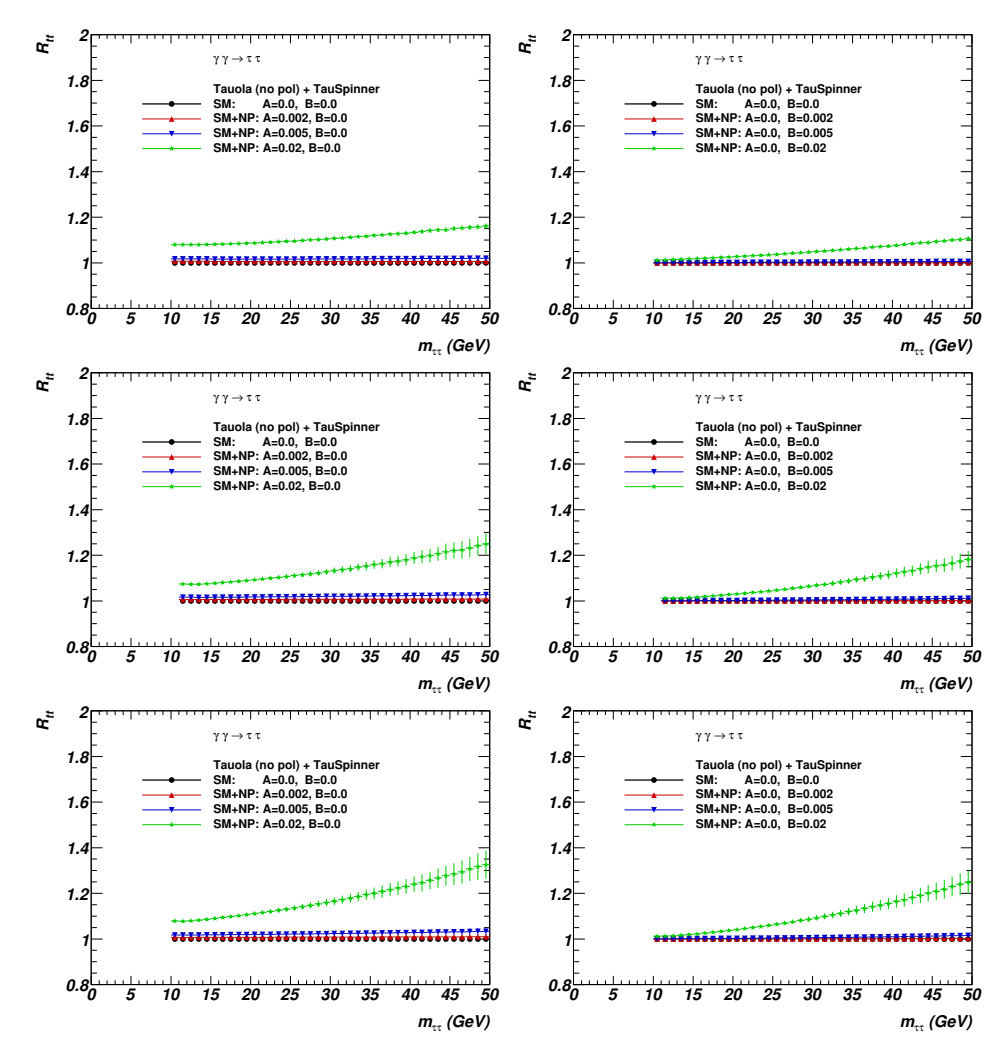


Fig. 2. Spin-averaged element R_{tt} as a function of $m_{\tau\tau}$: integrated over the full phase space (top plots), restricted to $\theta = \pi/3 \times [0.8 - 1.2]$ (middle plots), and restricted to $\theta = 2\pi/3 \times [0.8 - 1.2]$ (bottom plots). Compared are SM and SM+NP with six models: A = 0.002, 0.005, 0.02 and B = 0 (left column) and A = 0.0, B = 0.002, 0.005, 0.02 (right column). Curves marked with \star (shown in green) always denote the largest anomalous moment: A = 0.02 (left column), or B = 0.02 (right column).

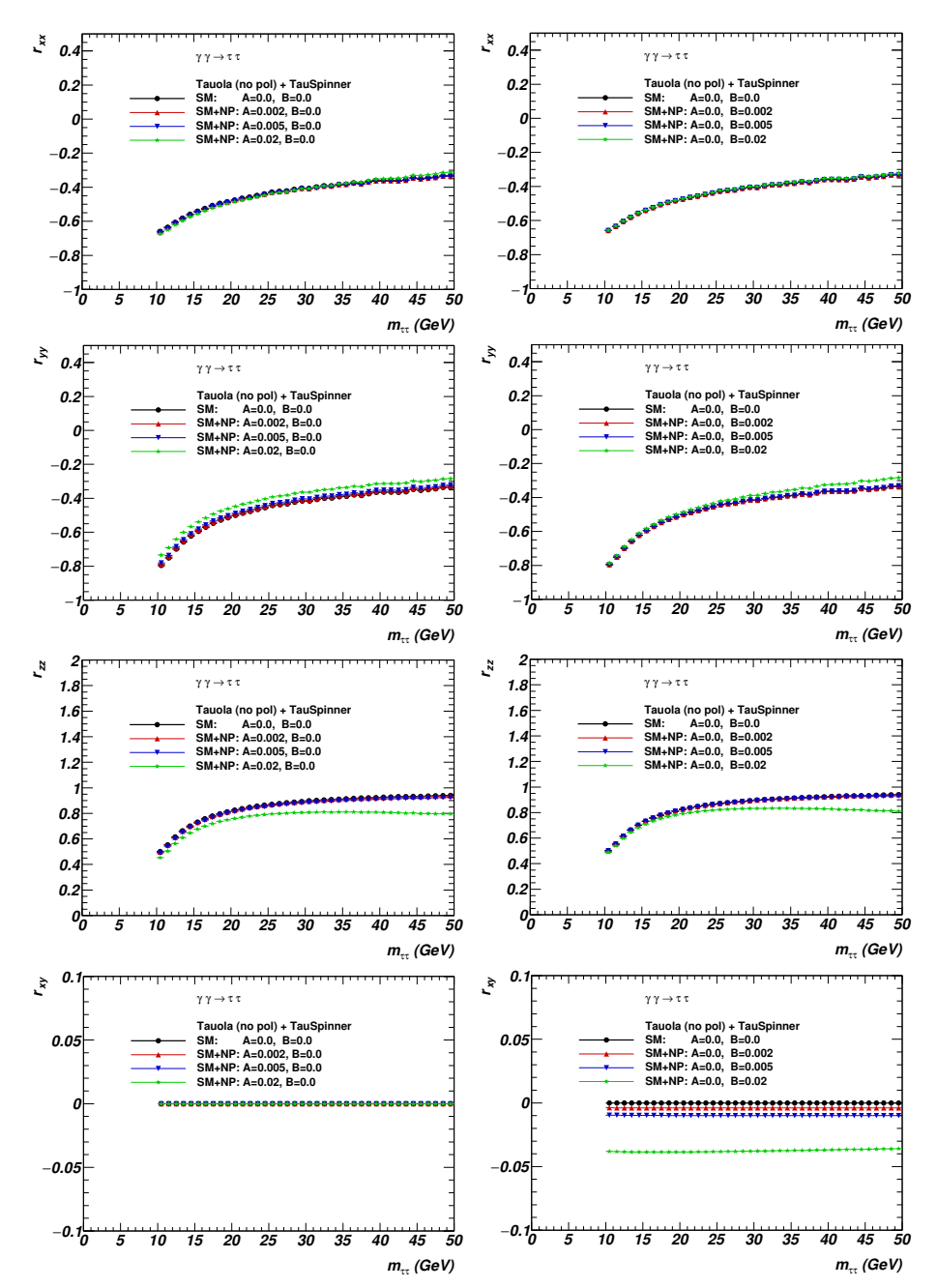


Fig. 3. Spin-correlation matrix elements r_{xx} , r_{yy} , r_{zz} , and r_{xy} as functions of $m_{\tau\tau}$. Notation is the same as in Fig. 2, except r_{xy} , these are elements with sizable SM contributions.

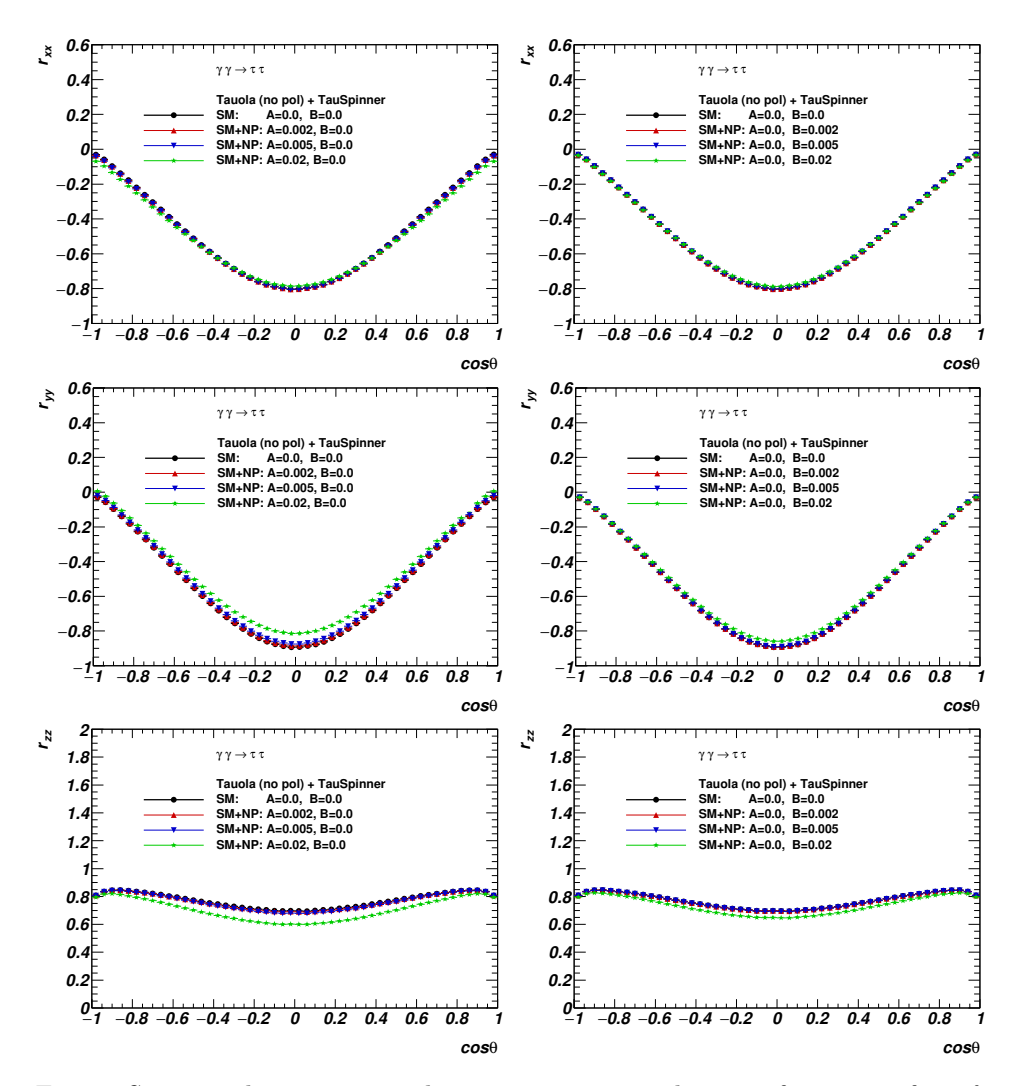


Fig. 4. Spin-correlation matrix elements r_{xx} , r_{yy} , and r_{zz} as functions of $\cos \theta$. Notation is the same as in Fig. 2. These elements have sizable contributions from the SM.

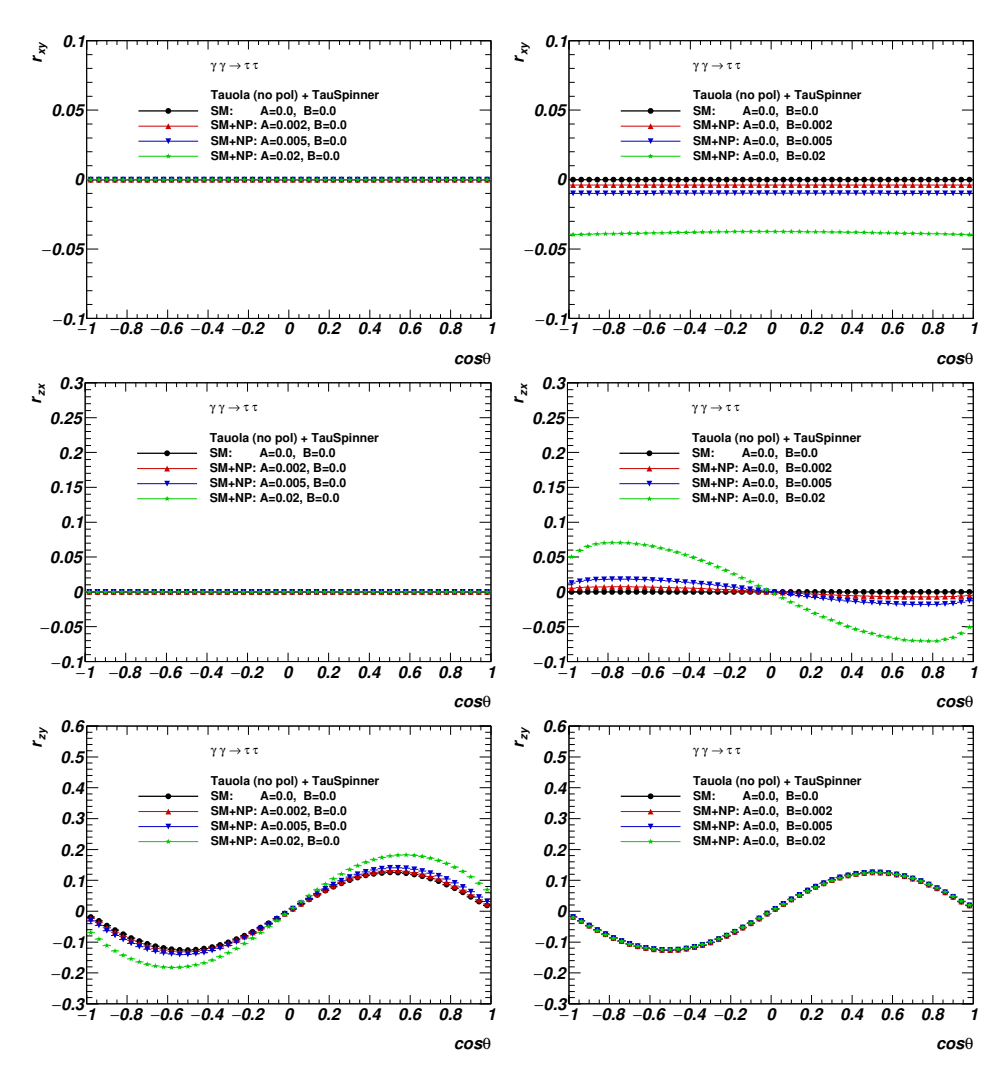


Fig. 5. Spin-correlation matrix elements r_{xy} , r_{zx} , and r_{zy} as functions of $\cos \theta$. Notation is the same as in Fig. 2. Elements r_{xy} , r_{zx} have negligible SM contributions, but non-negligible NP ones, while r_{zy} is sizable already in the SM and attains additional contribution from NP.

We can conclude that the SM spin correlations are in many cases sizable and dominate over the impact from the dipole moments. But it is not always the case, for example, r_{xy} and r_{zx} at certain angles are zero in the SM, but attain contribution from NP. That may give some hints on how to optimize the choice of observables and minimize background, at the same time underlying the importance of spin correlations as a possible bias for the cross-section R_{tt} -based signatures.

4.2. Spin effects in the
$$\tau^{\pm} \to \pi^{\pm} \nu_{\tau}$$
 decay channels

Let us now turn attention to distributions constructed from the observable τ -decay products. In Fig. 6, the effect of spin correlations is shown as in the SM (A=0, B=0) on a few kinematical variables: transverse momenta of the pions, $p_{\rm T}^{\pi}$, ratio E_{π}/E_{τ} , and ratio of invariant mass of $\pi^{+}\pi^{-}$ system to $\tau^{+}\tau^{-}$ system, $m_{\pi\pi}/m_{\tau\tau}$. The $p_{\rm T}^{\pi}$ and the E_{π}/E_{τ} distributions are rather insensitive to the spin correlations in the $\gamma\gamma \to \tau\tau$ process. However, for the kinematical observable constructed from the four-momenta of both pions, $m_{\pi\pi}/m_{\tau\tau}$, the effect is apparent. The change in the shape of the distribution of $m_{\pi\pi}/m_{\tau\tau}$ is at the level of 10–20% in a wide range around $m_{\pi\pi}/m_{\tau\tau}=0.5$.

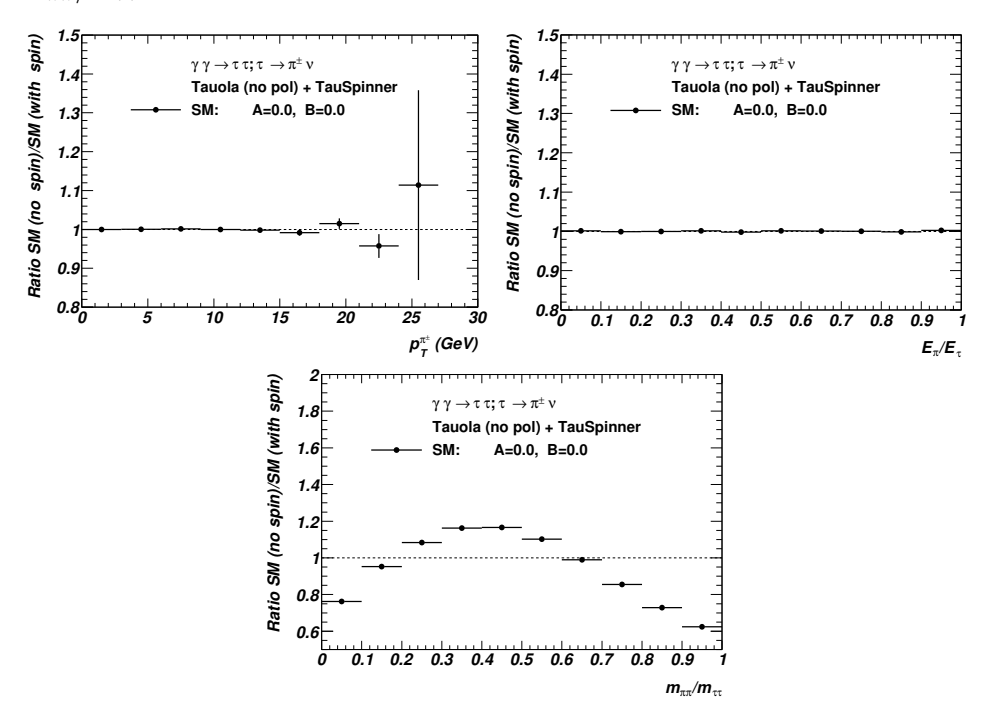


Fig. 6. Spin-correlation effects for the case of τ lepton decays: $\tau^+ \to \pi^+ \bar{\nu}_{\tau}$ and $\tau^- \to \pi^- \nu_{\tau}$. The ratio SM (no spin correlations)/SM (with spin correlations) is shown.

Figure 7 shows the effect of SM+NP extension in the normalisation and spin correlations. Plots of the ratio (SM+NP)/SM are shown, both including spin correlations. Once integrated over the full phase space, the impact from SM+NP extension is mostly due to change in the cross section. However, we also observe some change in the shape of the $p_{\rm T}^{\pi}$ distribution, with the ratio SM+NP to SM rising with the increasing $p_{\rm T}^{\pi}$ for A=0.02 or B=0.02. Some shape effect is also visible in the $m_{\pi\pi}/m_{TT}$ distribution for A=0.02.

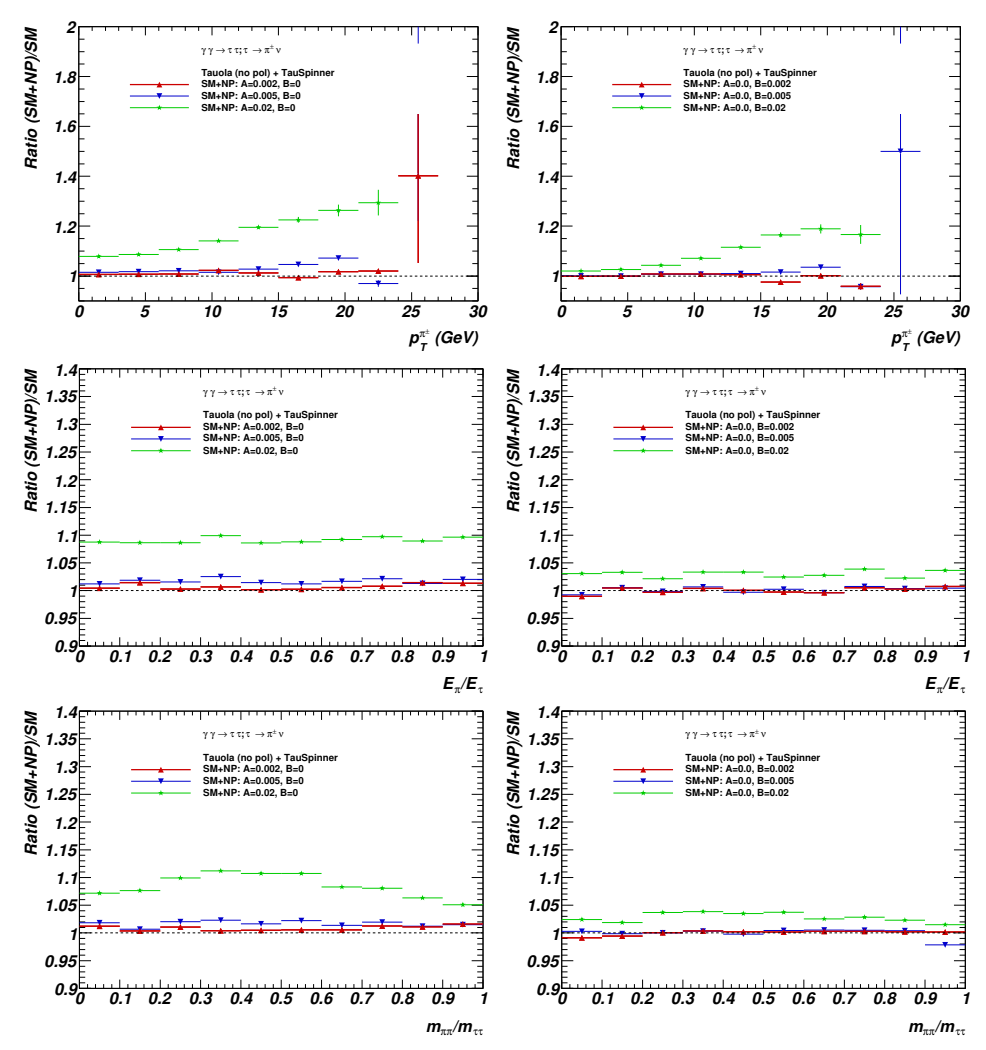


Fig. 7. The $p_{\rm T}^{\pi}$, E_{π}/E_{τ} , and $m_{\pi\pi}/m_{\tau\tau}$ distributions. Both τ leptons decay via $\tau^{\pm} \to \pi^{\pm} \nu_{\tau}$. Notation is the same as in Fig. 2.

4.3. Spin effects in the $\tau^{\pm} \to \rho^{\pm} \nu_{\tau}$ decay channels

In Fig. 8, the effect of spin correlations is shown as in the SM (A=0, B=0) on a few kinematical variables: transverse momenta of charged pions $p_{\rm T}^{\pi}$, the ratio E_{ρ}/E_{τ} , the ratio $Y=E_{\pi^{\pm}}/E_{\rho}$, and the ratio of invariant mass of the $\rho^{+}\rho^{-}$ system to $\tau^{+}\tau^{-}$ system $m_{\rho\rho}/m_{\tau\tau}$. Examples of the ratio (SM no spin)/(SM with spin) are shown. The $p_{\rm T}^{\pi}$ distribution and distributions of E_{ρ}/E_{τ} , $E_{\pi^{\pm}}/E_{\rho}$ are rather insensitive to the spin correlations in the $\gamma\gamma \to \tau\tau$ process. However, for kinematical observables constructed from the fourmomenta of both ρ mesons, like $m_{\rho\rho}/m_{\tau\tau}$, the effect is apparent. The change in the shape of the $m_{\rho\rho}/m_{\tau\tau}$ distribution is at the level of 10–15% in a wide range around $m_{\rho\rho}/m_{\tau\tau}=0.5$.

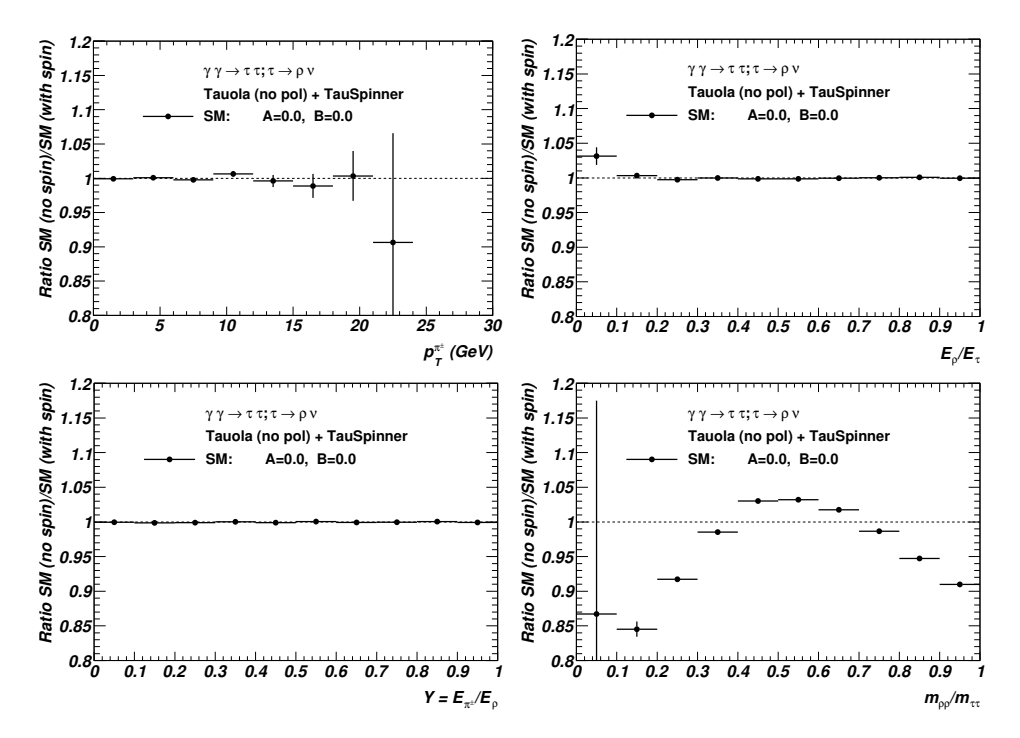


Fig. 8. Spin-correlation effects for the τ -lepton decays: $\tau^+ \to \rho^+ \bar{\nu}_{\tau}$ and $\tau^- \to \rho^- \nu_{\tau}$. Results for the ratio SM (no spin correlations)/SM (with spin correlations) are shown.

Figure 9 shows the effect of SM+NP extension in the normalisation and spin correlations. Shown are the plots of the ratio (SM+NP)/SM, both including spin correlations. Once integrated over the full phase-space, the impact from SM+NP extension is mostly due to the change of the cross section. However, we also observe some change in the shape of $p_{\rm T}^{\pi}$ distribution, with the ratio SM+NP to SM rising with increasing $p_{\rm T}^{\pi}$ for A=0.02 or

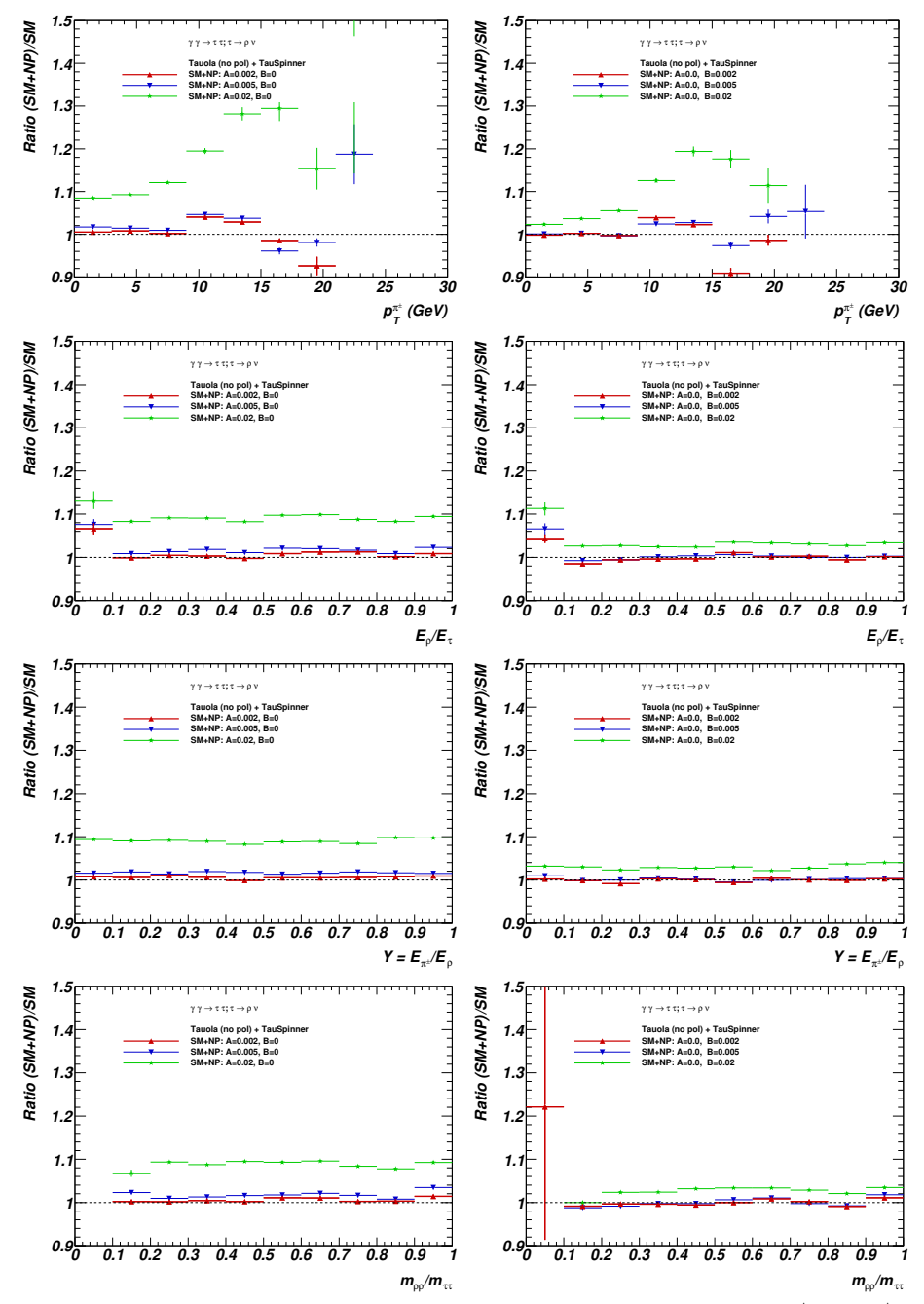


Fig. 9. Kinematical distributions for both τ leptons decaying via $\tau^{\pm} \to \rho^{\pm} \nu_{\tau}$. Notation is the same as in Fig. 2.

B = 0.02. Some shape effects are also visible for the $m_{\rho\rho}/m_{\tau\tau}$ distribution with A = 0.02. However, without a careful detector study, it is not clear how useful the effects can be for the measurements aiming at sensitivity to NP.

4.4. Spin effects in the decay channels
$$\tau^{\pm} \to \pi^{\pm} \nu_{\tau}$$
, $\tau^{\mp} \to \mu^{\mp} \nu_{\tau} \nu_{\mu}$

In the leptonic τ decays, the two neutrinos escape detection. That is why events with the leptonic τ -decay channels may be more difficult to interpret. Nonetheless, the leptonic decays represent more than 30% of τ -decay rate and are experimentally easier to trigger on, thus requiring some attention.

In Fig. 10, the effect of spin correlations is shown as in the SM (A=0, B=0) on a few kinematical variables: transverse momenta, $p_{\rm T}^{\mu}$ and $p_{\rm T}^{\pi}$, ratios E_{μ}/E_{τ} and E_{π}/E_{τ} , transverse momentum of the $\mu\pi$ system $p_{\rm T}^{\mu\pi}$ and the ratio of the invariant mass of the $\mu\pi$ system to that of $\tau^{+}\tau^{-}$ system, $m_{\mu\pi}/m_{\tau\tau}$. Some examples of the ratio (SM no spin)/(SM with spin) are shown. The $p_{\rm T}^{\mu}$, $p_{\rm T}^{\mu}$ distributions and distributions of the ratios E_{μ}/E_{τ} , E_{π}/E_{τ} are rather insensitive to the spin correlations in the $\gamma\gamma \to \tau\tau$ process. However, for the kinematical observables constructed from the four-momenta of both charged particles, π and μ , such as $p_{\rm T}^{\mu\pi}$ and $m_{\mu\pi}/m_{\tau\tau}$, the effect is apparent. The change in the shape of the $m_{\mu\pi}/m_{\tau\tau}$ distribution is at the level of 10–15% in a wide range around $m_{\mu\pi}/m_{\tau\tau}=0.5$.

Figures 11 and 12 show the effect of SM+NP extension in the normalisation and spin correlations. Shown are the ratios of (SM+NP)/SM, both including spin correlations. Again, once integrated over a full phase space, the impact from SM+NP extension is mostly due to the change in the cross section. However, we observe also some change in the shape of $p_{\rm T}^{\pi}$ distribution, with a ratio of SM+NP to SM rising with increasing $p_{\rm T}^{\pi}$, for both A=0.02 and B=0.02. Some shape effects are also visible in the $m_{\mu\pi}/m_{\tau\tau}$ distribution for A=0.02.

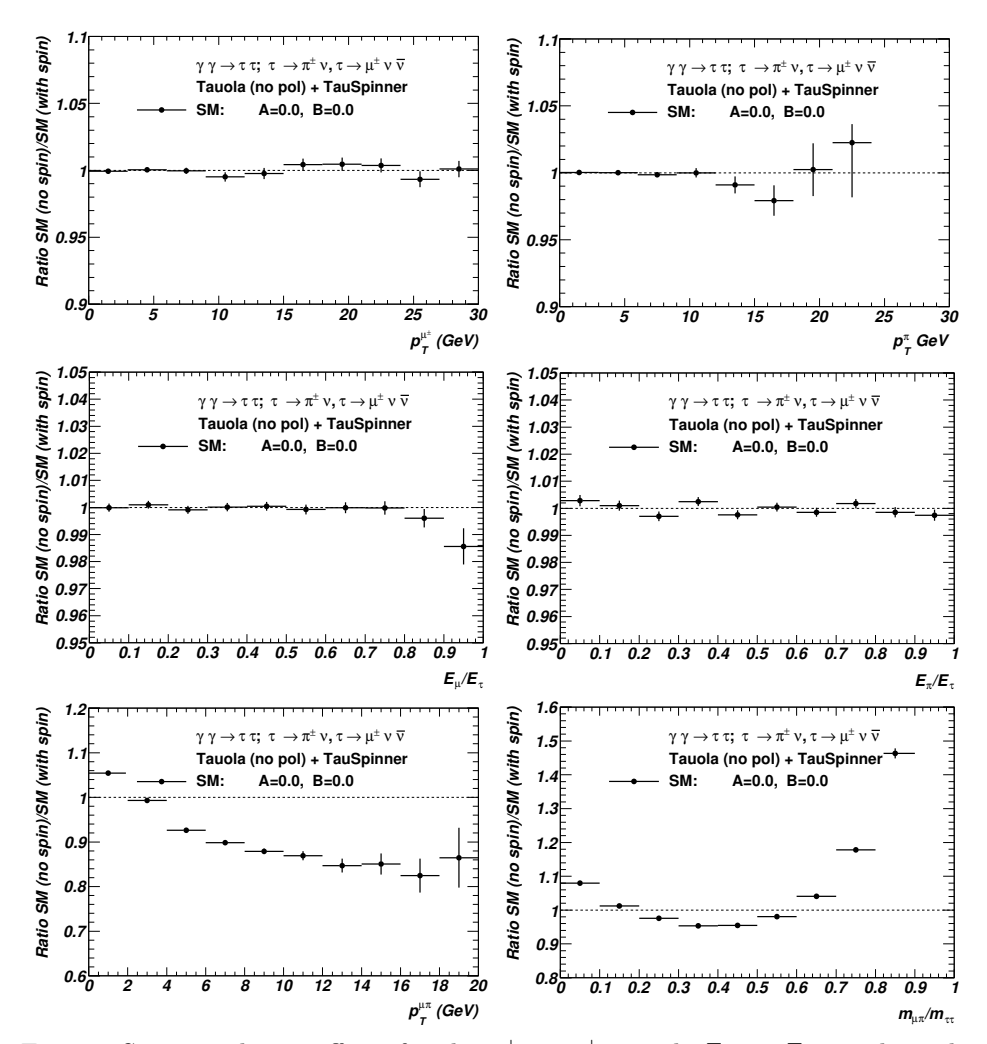


Fig. 10. Spin-correlation effects for the $\tau^{\pm} \to \pi^{\pm}\nu_{\tau}$ and $\tau^{\mp} \to \mu^{\mp}\nu_{\tau}\nu_{\mu}$ channels. Results for the ratios SM (no spin correlations)/SM (with spin correlations) are shown.

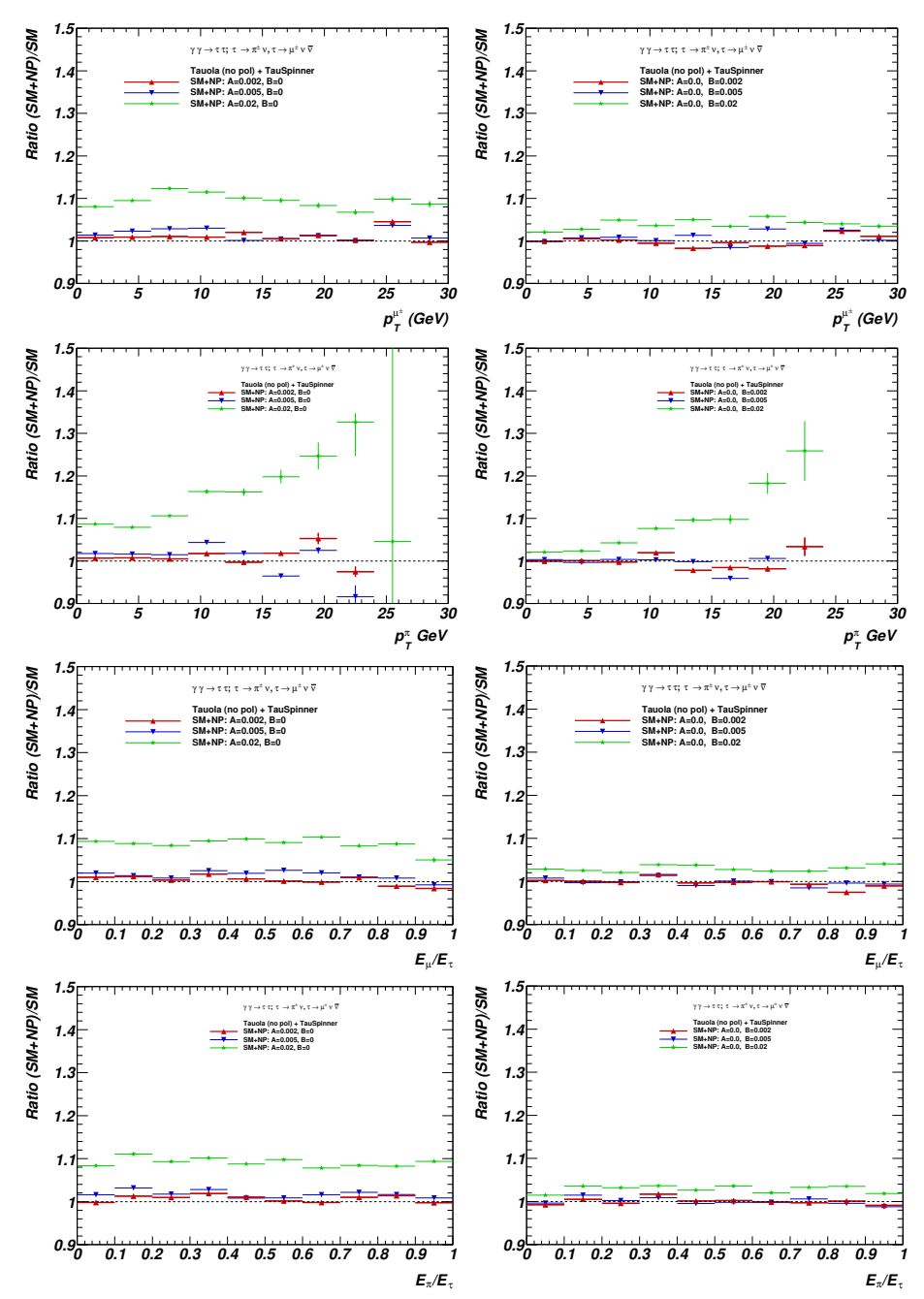


Fig. 11. Kinematical distributions for one τ decaying via $\tau^{\pm} \to \pi^{\pm} \nu_{\tau}$, and other τ decaying via $\tau^{\mp} \to \mu^{\mp} \nu_{\tau} \nu_{\mu}$. Notation is the same as in Fig. 2.

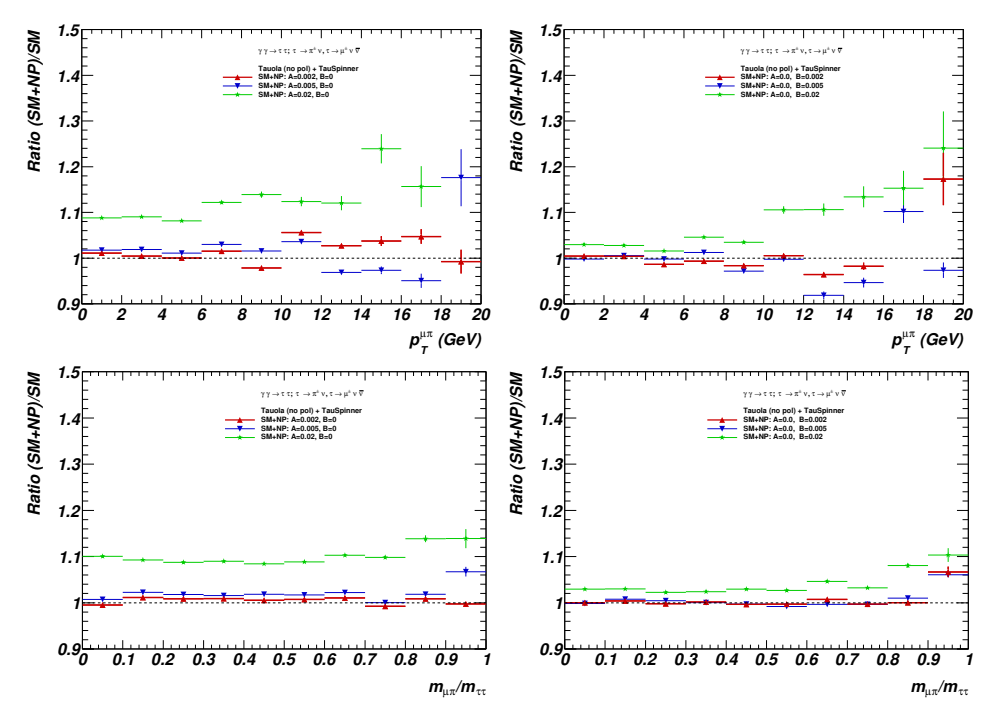


Fig. 12. Further kinematical distributions for one τ decaying via $\tau^{\pm} \to \pi^{\pm} \nu_{\tau}$, and other τ decaying via $\tau^{\mp} \to \mu^{\mp} \nu_{\tau} \nu_{\mu}$. Notation is the same as in Fig. 2.

5. Summary and outlook

The effects of $\gamma\gamma$ parton-level contributions to τ -pair production in pp and PbPb collisions at the LHC are of interest not only in themselves, but also for evaluating possible improvement in sensitivity to constraining anomalous electric and magnetic dipole moments from the spin effects.

In the present paper, we have addressed the ways to implement effects of such New Physics interactions with the attributions to the event weights. Physics input is presented with the help of the parton-level $2 \to 2$ processes, where anomalous terms due to electric and magnetic dipole moments are included. Such a solution can be applied directly to any other model of NP interactions, provided it can be encapsulated into form-factors as in Eq. (3) (in general, rather straightforward recalculation of functions used by the algorithm is needed). The collection of plots to illustrate sensitivity to dipole moments of the spin-correlation matrix elements is presented. Examples, sensitive to spin, observable distributions are evaluated, however, without sufficiently detailed evaluation of detector responses, they require refinements. We have first chosen $\tau^{\pm} \to \pi^{\pm} \nu_{\tau}$ decays as they are the sim-

plest to interpret. Then we turned to $\tau^{\pm} \to \rho^{\pm} \nu_{\tau}$, because sensitivity to the transverse spin is observable from the visible decay products only. In the end, we have provided examples, where one of the τ leptons decays through the leptonic channel. In this case, interpretation is difficult (due to extra neutrino escaping detection), nonetheless, such configurations represent almost half of all events. Such events may also be useful for the Machine Learning applications. Therefore, reference distributions may be of interest. Further exploration of sensitivity requires the active participation of physicists involved in the experimental analysis.

Some details on how TauSpinner algorithm for event reweighting with the new options introduced are provided as well.

This project was supported in part by funds of the National Science Centre (NCN), Poland, grant No. 2023/50/A/ST2/00224 and of COPIN-IN2P3 collaboration with LAPP-Annecy.

Appendix A

TauSpinner: technical details

Let us recall the steps of the TauSpinner initialisation and provide a user guide for configuring the $\gamma\gamma \to \tau\tau$ component of the spin and production weights.

With the available implementation, weights are calculated assuming that the $\tau\tau$ final state is a product of either $\bar{q}q$ or $\gamma\gamma$ scattering. The calculations of corresponding R_{ij} elements of the spin-correlation matrix are invoked and the proportion, with which each of the processes contributed to the sum in Eq. (20), depends on the parametrisation of the structure functions $f(x_1,\ldots), f(x_2,\ldots)$. Those represent probabilities of finding in the colliding beam partons (quark, gluon or photon), carrying momentum fractions x_1 , x_2 .

In the case of the proton–proton beams, the probabilities $f(x_1,...)$, $f(x_2,...)$ will be taken from a PDFs library, e.g. parametrisations of [24, 25] include also the photon structure functions. The parametrisation used should be indicated during initialisation. For the PbPb collision, the library parametrising photon flux is not available, and a user setup will be required. For example, by hand, the $\gamma\gamma$ contribution to R_{ij} can be taken in a fixed proportion to the summed over flavours $\bar{q}q$ one.

Package distribution

The tarball of the package can be downloaded from the web page: https://tauolapp.web.cern.ch/tauolapp/

The TauSpinner package is distributed in the same tarball as the TAUOLA package, a library for simulating τ decay, as they share several components of the code, interfaces, and tests.

The installation script is prepared and is located in the main directory: tauola/install-everything.sh

which is installing both TAUOLA/TauSpinner but also other packages needed for execution of the code and/or examples: HepMC, LHAPDF, PHOTOS, MCTESTER, Pythia. You can comment it out and provide links with details of already existing installations in your own environment.

The examples of use with a short README can be found in the directory tauola/TauSpinner/examples of the distributed tarball. In particular, files

read_particles_from_TAUOLA.cxx
tau-reweight-test.cxx

provide a good starting point.

Initialization

The user is required to configure both $\bar{q}q \to \tau\tau$ and $\gamma\gamma \to \tau\tau$ processes. If the $\gamma\gamma$ process will overly contribute, details of the configuration used for $\bar{q}q$ process are not relevant.

For both $\bar{q}q$ and $\gamma\gamma$ processes, the flag ifkorch = 1 is mandatory, as it invokes a consistent flow of the R_{ij} and final weight calculations. Details of the implementation of corresponding matrix elements were given in [18] with extension to higher-order terms for electromagnetic dipole moments as discussed in Section 2 of the present paper. The flag iqed = 0 switches off the SM component A0 of the magnetic dipole moment, then the total A, B values can be defined by the user. At the initalisation step, the user is required to provide values of the dipole moments used for sample generation A0i, B0i and those of the NP model for which weight will be calculated Ai, Bi. It is also required that the user provides the proportion of the $\gamma\gamma$ process with respect to the $\bar{q}q$ one, at generation GAMfraci and for the desired NP model GAMfrac2i. If only the $\gamma\gamma$ process is considered, this proportion should be set to be excessively large to make the quark—antiquark contribution negligible; in the example below, it is set to 10^6 .

We expect that in a standard usage, the initialisation of parameters will be performed once. However, re-initialisation of the parameters is possible on event-by-event base. One can change, e.q. the setting of EW corrections or dipole moments and process the same event several times for weight calculation. The ratio of the weights calculated, e.g. for the two sets of parameters and the same event, can then be used to estimate interesting properties of NP models.

Below shown is a snippet of the initialisation, the user code should follow, e.q. after the example from:

tauola/TauSpinner/examples/tau-reweight-test.cxx

```
// initialisation of main flow of TauSpinner
  double CMSENE = 13000.0; // center of mass system energy
                          // used in PDF calculation. For p p collisions only
  bool Ipp = true;
                          // for $pp$ collisions, the only option implemented
                          // but gam gam events from Pb Pb events can be also
                          // processed, detail
  int Ipol = 0; // are input samples polarized?
   int nonSM2 = 1; // are we using nonSM calculations?
  int nonSMN = 0; // If we are using nonSM calculations we may want corrections
                  // to shapes only: y/n (1/0)
  TauSpinner::initialize_spinner(Ipp, Ipol, nonSM2, nonSMN, CMSENE);
// initialization for Dizet electroweak tables, here you specify location
// where the tables are present, default: in your run directory
// for more documentation see arXiv:2012.10997, arXiv:1808.08616
  char* mumu="table.mu";
  char* downdown= "table.down";
  char* upup= "table.up";
  int initResult=initTables(mumu,downdown,upup);
// initialisation for EW parameters
// for more documentation see arXiv:2012.10997, arXiv:1808.08616
  double SWeff=0.2315200;
  double DeltSQ=0.;
  double DeltV=0.;
  double Gmu=0.00001166389;
  double alfinv=128.86674175;
  int keyGSW=1;
  double AMZi=91.18870000;
  double GAM=2.49520000;
  ExtraEWparamsSet(AMZi, GAM, SWeff, alfinv,DeltSQ, DeltV, Gmu,keyGSW);
// initialisation for the qqbar ->tautau matrix elements
// dipole moments and weak dipole moments are set to 0.0 in the qbarq->tautau ME
// flags relevant here are:
  int ifkorch = 1; // global flag to switch on ME calculations of arXiv:2307.03526
```

```
// initialisation for the gamma gamma ->tautau matrix elements
// works only if global flag ifkorch = 1
// artificial weight for fraction of gamgam vs qbar process, if not calculated
// directly from structure functions proportions
double GAMfraci = 1000000.0;
double GAMfrac2i = 1000000.0;
// values for dipole moments used in generated sample (A0i, B0i)
// and in the model for which weight is calculated (Ai, Bi)
double A0i = 0.0;
double B0i = 0.0;
double Bi = 0.001177;
double Bi = 0.0;
initialize_gamagama(GAMfraci, GAMfrac2i, A0i, B0i, Ai, Bi);
```

Calculation of event weights

The spin correlations matrix R_{ij} (coded in FORTRAN) is used by the weight calculating method (coded in C++). The function dipolgamma_(iqed, E, theta, A0, B0, Rij) has several input parameters iqed, E, theta, A0, B0, and output matrix Rij. The E, theta denote, respectively, the energy of the scattering photon in the $2 \to 2$ parton level centre-of-mass frame and scattering angle of the outgoing τ lepton with respect to photon beam direction, also in this frame⁷. The A0, B0 denote magnetic and electric moments. The iqed flag switches the OFF/ON contribution to A0 from the SM $A(0)_{\rm SM} = 1.17721(5) \times 10^{-3}$ of the anomalous magnetic dipole moment, as calculated in [9].

For each event, which is read from the input_file by:

the calculation of the spin weight WTspin and the corresponding relative change to the cross section WTprod, due to NP values of dipole moments, can be invoked.

By definition, always an average of spin weight $\langle WTspin \rangle = 1.0$. To quantify the impact on a particular kinematical distribution of including

⁷ The elements of the Rij matrix are calculated by routines dipolgamma_ and dipolqq_, respectively, for $\gamma\gamma$ and antiquark–quark processes. They are provided in the TAUOLA/TauSpinner/src/initwksw.f file. In addition to calculation, the frame reorientation is provided in these FORTRAN interfacing routines (Eq. (18)). Also, the change of index convention from FORTRAN 1,2,3,4 to C++ 0,1,2,3 is introduced. Finally, a minus sign originating from τ^+ V+A coupling instead of τ^- V-A is introduced in the C++ code. This also explains a sign change in R_{yy} versus publication [18].

spin correlations for a given (SM+NP) model with respect to one used in the generated sample, one should use the product $WTspin \cdot WTprod$ when filing histograms. By construction, for model with A0i, B0i calculated WTprod = 1.0. It means that only a relative change in the cross section, not the absolute one, can be accessed with the present implementation in TauSpinner.

Accessing internal variables

Several functions (*getters*) are available to access the prepared internal variables. In particular, for each event, with the methods

```
getZgamParametersTR(Rxx, Ryy, Rxy, Ryx);
getZgamParametersL(Rzx, Rzy, Rzz, Rtx, Rty, Rtz);
```

the set of R_{ij} matrix components can be accessed, as they might be of interest for monitoring purposes.

Appendix B

Elements of the $\gamma\gamma \to \tau\tau$ spin-correlation matrix

In this appendix, the elements of the matrix R_{ij} are presented in the form which is actually used in the FORTRAN code. Physics-wise, they do not differ from the ones of Eq. (7)

$$R_{11} = \frac{e^4}{4\gamma^4 (1 - \beta^2 \cos^2 \theta)^2} \Big[\beta^2 \gamma^2 \Big(-8 + 2 (4 + 8A + 10A^2 + 4A^3 + A^4 + 2(-1 + A)(3 + A)B^2 + B^4 \Big) \gamma^2 - 4 (-4B^2 + (A^2 + B^2)^2) \gamma^4 + 3 (A^2 + B^2)^2 \gamma^6 \Big) \cos^2 \theta + (A^2 + B^2)^2 \beta^6 \gamma^8 \cos^6 \theta + \beta^4 \gamma^4 \cos^4 \theta \Big(-4 + \gamma^2 \Big(-8B^2 - (A^2 + B^2)^2 (-1 + 2\gamma^2) \Big) - (A^2 + B^2)^2 \gamma^2 (-1 + \gamma^2) \cos 2\theta \Big) + \frac{1}{2} (-16 - 8 (-1 + A(2 + A) + 4B^2) \gamma^2 - (4 (A(2 + A)(2 + A(4 + A)) + 2(-2 + A(3 + A))B^2 + B^4) + (2 + 4A + 4A^2 + 2A^3 + A^4 + 2 (1 + A + A^2) B^2 + B^4) \beta^2) \gamma^4 + (-8B^2 + 2(A(2 + A) + B^2)^2 + (-2 + (-2 + A)A + B^2) (A^2 + B^2) \beta^2) \gamma^6 - (A^2 + B^2)^2 \beta^2 \gamma^8 - 2 (-1 + \gamma^2) (2(1 + A)\gamma + (A^2 + B^2) \gamma^3)^2 \cos 2\theta + \beta^2 \gamma^4 (2 + 4A + 4A^2 + 2A^3 + A^4 + 2B^2 + 2AB^2 + 2A^2B^2 + B^4 - (-2 + (-2 + A)A + B^2) (A^2 + B^2) \gamma^2 + (A^2 + B^2)^2 \gamma^4) \cos 4\theta \Big) \Big]. (B.1)$$

$$R_{22} = \frac{e^4}{4\gamma^4 (1 - \beta^2 \cos^2 \theta)^2} \Big[-8 + (8 - 16B^2) \gamma^2 -2 (2 + 4A^3 + A^4 - 6B^2 + B^4 + 4A (2 + B^2) + 2A^2 (5 + B^2)) \gamma^4 +2 (A^4 - 4B^2 + 2A^2B^2 + B^4) \gamma^6 - (A^2 + B^2)^2 \gamma^8 +\beta^2 \gamma^2 (-8 + 2 (4 + 4A^3 + A^4 - 6B^2 + B^4 + 4A (2 + B^2) +2A^2 (5 + B^2)) \gamma^2 - 4 (A^4 - 4B^2 + 2A^2B^2 + B^4) \gamma^4 +3 (A^2 + B^2)^2 \gamma^6 \Big) \cos^2 \theta - \beta^4 \gamma^4 (4 + 8B^2 \gamma^2 + A^4 \gamma^2 (-2 + 3\gamma^2) +2A^2 B^2 \gamma^2 (-2 + 3\gamma^2) + B^4 \gamma^2 (-2 + 3\gamma^2) \Big) \cos^4 \theta + (A^2 + B^2)^2 \beta^6 \gamma^8 \cos^6 \theta \Big].$$
(B.2)

$$R_{12} = \frac{e^4}{16\gamma^2 (1 - \beta^2 \cos^2 \theta)^2} B\beta \left[-32 + 32A - 48\gamma^2 - 192A\gamma^2 - 52A^2\gamma^2 - 20B^2\gamma^2 + 28\beta^2\gamma^2 + 120A\beta^2\gamma^2 + 27A^2\beta^2\gamma^2 + 3B^2\beta^2\gamma^2 + 112A\gamma^4 + 44A^2\gamma^4 + 12B^2\gamma^4 - 172A\beta^2\gamma^4 - 65A^2\beta^2\gamma^4 - 9B^2\beta^2\gamma^4 + 72A\beta^4\gamma^4 + 27A^2\beta^4\gamma^4 + 3B^2\beta^4\gamma^4 + 4\left(8 + \left(-4 + 8\beta^2 + B^2\left(3 + \beta^2\right)\right)\gamma^2 + B^2\left(-1 - 2\beta^2 + \beta^4\right)\gamma^4 + 4A\left(2 + \left(-6 + 9\beta^2\right)\gamma^2 + \left(5 - 12\beta^2 + 6\beta^4\right)\gamma^4\right) + A^2\gamma^2\left(-5 + 7\gamma^2 + 9\beta^4\gamma^2 + \beta^2\left(9 - 18\gamma^2\right)\right)\cos 2\theta + \beta^2\gamma^2\left(4 + B^2\left(1 + \left(1 + \beta^2\right)\gamma^2\right) + 4A\left(6 + \left(-5 + 6\beta^2\right)\gamma^2\right) + A^2\left(9 + \left(-7 + 9\beta^2\right)\gamma^2\right)\cos 4\theta \right].$$
(B.3)

$$R_{33} = -\frac{e^4}{4\gamma^4 (1 - \beta^2 \cos^2 \theta)^2} \left[-8 - 8 \left(-3 + 2B^2 \right) \gamma^2 - 2 \left(10 + 4A^3 + A^4 + B^4 - 4\beta^2 + 4A \left(2 + B^2 + 2\beta^2 \right) + 2A^2 \left(5 + B^2 + 2\beta^2 \right) + B^2 \left(-22 + 8\beta^2 \right) \right) \gamma^4 + 2 \left(4 + 3A^4 + 3B^4 - 4\beta^2 + 2A^2 \left(10 + 3B^2 - 8\beta^2 \right) - 4A^3 \left(-2 + \beta^2 \right) + 4B^2 \left(-4 + 3\beta^2 \right) - 4A \left(B^2 \left(-2 + \beta^2 \right) + 4 \left(-1 + \beta^2 \right) \right) \right) \gamma^6 + \left(A^4 \left(-5 + 2\beta^2 \right) + 2A^2 B^2 \left(-5 + 2\beta^2 \right) + B^2 \left(-16 \left(-1 + \beta^2 \right) + B^2 \left(-5 + 2\beta^2 \right) \right) \right) \gamma^8 - 2 \left(A^2 + B^2 \right)^2 \left(-1 + \beta^2 \right) \gamma^{10} + \gamma^2 \left(-2\gamma^2 \left(-1 + \gamma^2 \right) \left(2 + 2A + A^2 \gamma^2 + B^2 \gamma^2 \right)^2 + \beta^2 \left(-8 + 2 \left(4 + 4A^3 + A^4 - 14B^2 + B^4 + 4A \left(2 + B^2 \right) + 2A^2 \left(5 + B^2 \right) \right) \gamma^2 - 16 \left(A + 3A^3 + A^4 + 3AB^2 + B^2 \left(-16 + 11B^2 \right) + 2A^2 \left(2 + B^2 \right) \right) \gamma^4 + \left(16A^3 + 11A^4 + 16AB^2 + B^2 \left(-16 + 11B^2 \right) + 2A^2 \left(8 + 11B^2 \right) \right) \gamma^6 - 2 \left(A^2 + B^2 \right)^2 \gamma^8 \right) + 4\beta^4 \gamma^4 \left(2 - 2A^3 \left(-3 + \gamma^2 \right) + B^2 \left(-2 + 6\gamma^2 \right) + A^4 \left(1 - \gamma^2 + \gamma^4 \right) + B^4 \left(1 - \gamma^2 + \gamma^4 \right) \right) \right) \cos^2 \theta - \beta^2 \gamma^4 \left(\beta^2 \left(4 - 2 \left(-4 - 8A + A^4 - 8B^2 + B^4 + 2A^2 \left(-2 + B^2 \right) \right) \gamma^2 + \left(16A^3 + 7A^4 + 16AB^2 + 7B^4 + 2A^2 \left(8 + 7B^2 \right) \right) \gamma^4 + 2 \left(A^2 + B^2 \right)^2 \gamma^6 \right) + 2\beta^4 \gamma^4 \left(-4A^3 - 4AB^2 + A^4 \left(-1 + \gamma^2 \right) + 2A^2 \left(-2 + B^2 \left(-1 + \gamma^2 \right) \right) + B^2 \left(4 + B^2 \left(-1 + \gamma^2 \right) \right) \right) - 4\gamma^2 \left(2 + 2A^3 \left(1 + \gamma^2 \right) + 2B^2 \left(1 + \gamma^2 \right) + A^4 \left(1 - \gamma^2 + \gamma^4 \right) + 2A \left(2 + B^2 \left(1 + \gamma^2 \right) + 2A^2 \left(2 + \gamma^2 \right) + B^4 \left(1 - \gamma^2 + \gamma^4 \right) + 2A \left(2 + B^2 \left(1 + \gamma^2 \right) \right) + 2A^2 \left(2 + \gamma^2 \right) + B^2 \left(1 - \gamma^2 + \gamma^4 \right) \right) \right) \cos^4 \theta + \left(A^2 + B^2 \right)^2 \beta^4 \gamma^8 \left(2 - 2\gamma^2 + B^2 \left(1 - \gamma^2 + \gamma^4 \right) \right) \right) \cos^6 \theta \right].$$
(B.4)

$$\begin{split} R_{13} &= -\frac{e^4}{2\gamma (1-\beta^2 \cos^2\theta)^2} \cos\theta \left[4 - 4\beta^2 - 4B^2\beta^2 - 4\gamma^2 + 4B^2\gamma^2 \right. \\ &+ 4\beta^2\gamma^2 - 6B^2\beta^2\gamma^2 - 2B^4\beta^2\gamma^2 - 4B^2\gamma^4 + B^4\gamma^4 + 4B^2\beta^2\gamma^4 \\ &- B^4\gamma^6 + B^4\beta^2\gamma^6 + 4A \left(2 + \left(-2 + \beta^2 + B^2 \left(1 - 2\beta^2 \right) \right) \gamma^2 \right. \\ &+ B^2 \left(-1 + \beta^2 \right) \gamma^4 \right) + 4A^3\gamma^2 \left(1 - \gamma^2 + \beta^2 \left(-2 + \gamma^2 \right) \right) \\ &+ A^4 \left(\gamma^4 - \gamma^6 + \beta^2\gamma^2 \left(-2 + \gamma^4 \right) \right) + 2A^2 \left(-\left(-1 + \gamma^2 \right) \left(2 + 2\gamma^2 + B^2\gamma^4 \right) \right. \\ &+ \beta^2\gamma^2 \left(-3 + 2\gamma^2 + B^2 \left(-2 + \gamma^4 \right) \right) \right) - 2\beta^2\gamma^2 \left(2 \left(-1 + \beta^2 \right) \gamma^4 \right. \\ &+ \beta^2\gamma^2 \left(-3 + 2\gamma^2 + B^2 \left(-2 + \gamma^4 \right) \right) \right) - 2\beta^2\gamma^2 \left(2 \left(-1 + \beta^2 \right) \gamma^4 \right. \\ &+ B^4 \left(-1 + \left(-1 + \beta^2 \right) \gamma^2 \right) + A^4 \left(-1 + \gamma^2 + \left(-1 + \beta^2 \right) \gamma^4 \right) \\ &+ B^4 \left(-1 + \gamma^2 + \left(-1 + \beta^2 \right) \gamma^4 \right) + B^2 \left(-2 \left(1 + \gamma^2 \right) + \beta^2 \left(1 + 2\gamma^2 \right) \right) \\ &+ 2A \left(-2 + \beta^2 + B^2 \left(-1 + \left(-1 + \beta^2 \right) \gamma^2 \right) \right) + A^2 \left(-4 + \beta^2 - 2\gamma^2 \right. \\ &+ 2\beta^2\gamma^2 + 2B^2 \left(-1 + \gamma^2 + \left(-1 + \beta^2 \right) \gamma^4 \right) \right) \cos^2\theta \\ &+ \left(A^2 + B^2 \right)^2 \beta^4\gamma^4 \left(1 + \left(-1 + \beta^2 \right) \gamma^2 \right) \cos^4\theta \right] \sin\theta \,. \end{split} \tag{B.5}$$

REFERENCES

- N.F. Ramsey, «Electric-Dipole Moments of Particles», Annu. Rev. Nucl. Part. Sci. 32, 211 (1982).
- [2] H.-Y. Cheng, «CP-violating effects in leptonic systems», *Phys. Rev. D* 28, 150 (1983).
- [3] W. Bernreuther, O. Nachtmann, «CP-violating correlations in electron–positron annihilation into τ leptons», *Phys. Rev. Lett.* **63**, 2787 (1989); *Erratum ibid.* **64**, 1072 (1990).
- [4] Belle Collaboration (K. Inami *et al.*), «An improved search for the electric dipole moment of the τ lepton», *J. High Energy Phys.* **2022**, 110 (2022), arXiv:2108.11543 [hep-ex].
- [5] ATLAS Collaboration (G. Aad et al.), «Observation of the $\gamma\gamma \to \tau\tau$ Process in Pb+Pb Collisions and Constraints on the τ -Lepton Anomalous Magnetic Moment with the ATLAS Detector», Phys. Rev. Lett. 131, 151802 (2023), arXiv:2204.13478 [hep-ex].
- [6] CMS Collaboration (A. Tumasyan *et al.*), «Observation of τ -Lepton Pair Production in Ultraperipheral Pb–Pb Collisions at $\sqrt{s_{NN}} = 5.02$ TeV», *Phys. Rev. Lett.* **131**, 151803 (2023), arXiv:2206.05192 [nucl-ex].
- [7] Muon g-2 Collaboration (B. Abi *et al.*), «Measurement of the Positive Muon Anomalous Magnetic Moment to 0.46 ppm», *Phys. Rev. Lett.* **126**, 141801 (2021), arXiv:2104.03281 [hep-ex].
- [8] W. Bernreuther, A. Brandenburg, P. Overmann, «CP violation beyond the standard model and tau pair production in e^+e^- collisions», *Phys. Lett. B* **391**, 413 (1997); *Erratum ibid.* **412**, 425 (1997).
- [9] S. Eidelman, M. Passera, «Theory of the τ Lepton Anomalous Magnetic Moment», *Mod. Phys. Lett. A* **22**, 159 (2007), arXiv:hep-ph/0701260.
- [10] Z. Czyczula, T. Przedzinski, Z. Was, «TauSpinner program for studies on spin effect in tau production at the LHC», Eur. Phys. J. C 72, 1988 (2012), arXiv:1201.0117 [hep-ph].
- [11] T. Przedzinski, E. Richter-Was, Z. Was, «Documentation of TauSpinner algorithms: program for simulating spin effects in τ -lepton production at LHC», Eur. Phys. J. C 79, 91 (2019), arXiv:1802.05459 [hep-ph].
- [12] C. Bierlich et al., «A comprehensive guide to the physics and usage of PYTHIA 8.3», SciPost Phys. Codebasis 2022, 8 (2022), arXiv:2203.11601 [hep-ph].
- [13] Sherpa Collaboration (E. Bothmann *et al.*), «Event generation with Sherpa 2.2», *SciPost Phys.* 7, 034 (2019), arXiv:1905.09127 [hep-ph].
- [14] J. Kalinowski, W. Kotlarski, E. Richter-Wąs, Z. Wąs, «Production of τ lepton pairs with high $p_{\rm T}$ jets at the LHC and the TauSpinner reweighting algorithm», Eur. Phys. J. C 76, 540 (2016), arXiv:1604.00964 [hep-ph].

- [15] T. Przedziński, E. Richter-Wąs, Z. Wąs, «TauSpinner: a tool for simulating CP effects in $H \to \tau\tau$ decays at LHC», *Eur. Phys. J. C* **74**, 3177 (2014), arXiv:1406.1647 [hep-ph].
- [16] E. Richter-Was, Z. Was, «Documentation of TauSpinner approach for electroweak corrections in LHC $Z \rightarrow ll$ observables», *Eur. Phys. J. C* **79**, 480 (2019), arXiv:1808.08616 [hep-ph].
- [17] E. Richter-Was, Z. Was, «Adequacy of effective Born for electroweak effects and TauSpinner algorithms for high energy physics simulated samples», *Eur. Phys. J. Plus* **137**, 95 (2022), arXiv:2012.10997 [hep-ph].
- [18] S. Banerjee, A.Y. Korchin, E. Richter-Was, Z. Was, «Electron-positron, parton-parton, and photon-photon production of τ-lepton pairs: Anomalous magnetic and electric dipole moments spin effects», *Phys. Rev. D* 109, 013002 (2024), arXiv:2307.03526 [hep-ph].
- [19] S. Banerjee, A.Y. Korchin, Z. Was, «Spin correlations in τ -lepton pair production due to anomalous magnetic and electric dipole moments», *Phys. Rev. D* **106**, 113010 (2022), arXiv:2209.06047 [hep-ph].
- [20] M. Demirci, M.F. Mustamin, «One-loop electroweak radiative corrections to charged lepton pair production in photon-photon collisions», *Phys. Rev. D* 103, 113004 (2021), arXiv:2105.05340 [hep-ph].
- [21] S. Jadach, Z. Wąs, R. Decker, J.H. Kühn, «The τ decay library TAUOLA, version 2.4», *Comput. Phys. Commun.* **76**, 361 (1993).
- [22] A. Arbuzov et al., «The Monte Carlo Program KKMC, for the Lepton or Quark Pair Production at LEP/SLC Energies — Updates of electroweak calculations», Comput. Phys. Commun. 260, 107734 (2021), arXiv:2007.07964 [hep-ph].
- [23] N. Davidson et al., «Universal interface of TAUOLA: Technical and physics documentation», Comput. Phys. Commun. 183, 821 (2012), arXiv:1002.0543 [hep-ph].
- [24] S.R. Klein et al., «STARlight: A Monte Carlo simulation program for ultra-peripheral collisions of relativistic ions», Comput. Phys. Commun. 212, 258 (2017), arXiv:1607.03838 [hep-ph].
- [25] CTEQ-TEA Collaboration (K. Xie et al.), «Photon PDF within the CT18 global analysis», Phys. Rev. D 105, 054006 (2022), arXiv:2106.10299 [hep-ph].